Annu. Rev. Immunol. 1999. 17:435–66

THE STRUCTURAL BASIS OF T CELL ACTIVATION BY SUPERANTIGENS

Hongmin Li,[#] Andrea Llera,[#] Emilio L. Malchiodi,[#,] and Roy A. Mariuzza[#]*

[#]Center for Advanced Research in Biotechnology, University of Maryland Biotechnology Institute, Rockville, Maryland 20850, and [*]Instituto de Estudios de la Inmunidad Humoral, CONICET, Catedra de Inmunolgia, FFyB, UBA, 1113 Buenos Aires, Argentina; e-mail: mariuzza@indigo2.carb.nist.gov

KEY WORDS: staphylococcal enterotoxins, T cell receptor, T cell stimulation, three-dimensional structure

ABSTRACT

Superantigens (SAGs) are a class of immunostimulatory and disease-causing proteins of bacterial or viral origin with the ability to activate large fractions (5–20%) of the T cell population. Activation requires simultaneous interaction of the SAG with the Vβ domain of the T cell receptor (TCR) and with major histocompatibility complex (MHC) class II molecules on the surface of an antigen-presenting cell. Recent advances in knowledge of the three-dimensional structure of bacterial SAGs, and of their complexes with MHC class II molecules and the TCR β chain, provide a framework for understanding the molecular basis of T cell activation by these potent mitogens. These structures along with those of TCR-peptide/MHC complexes reveal how SAGs circumvent the normal mechanism for T cell activation by peptide/MHC and how they stimulate T cells expressing TCR β chains from a number of different families, resulting in polyclonal T cell activation. The crystal structures also provide insights into the basis for the specificity of different SAGs for particular TCR β chains, and for the observed influence of the TCR α chain on SAG reactivity. These studies open the way to the design of SAG variants with altered binding properties for TCR and MHC for use as tools in dissecting structure-activity relationships in this system.

0732-0582/99/0410-0435$08.00

INTRODUCTION

T lymphocytes recognize a wide variety of antigens through highly diverse cell-surface glycoproteins known as T cell receptors (TCRs). These disulfide-linked heterodimers are composed of α and β, or γ and δ, chains that have variable (V) and constant (C) regions that are structurally homologous to those of antibodies (1, 2). Unlike antibodies, however, which recognize antigen alone, $\alpha\beta$ TCRs recognize antigen only in the form of peptides bound to major histocompatibility complex (MHC) molecules. In addition, TCRs interact with a class of viral or bacterial proteins known as superantigens (SAGs), which stimulate T cells bearing particular Vβ elements, resulting in the massive release of T cell–derived cytokines such as interleukin (IL)-2 and tumor necrosis factor (TNF) β, generally followed by the eventual disappearance or inactivation of responding T cells (3–4). Activation of the T cell requires simultaneous interaction of the SAG with the TCR and with MHC class II molecules on an antigen-presenting cell (APC).

The best-characterized group of SAGs belongs to the so-called pyrogenic toxin SAG family, which includes the staphylococcal enterotoxins (SE)A through I (except F), staphylococcal toxic shock syndrome toxin-1 (TSST-1), streptococcal superantigen (SSA), and streptococcal pyrogenic exotoxins (SPE)A-C and -F (6–8). These bacterial SAGs have in common the following characteristics: (*a*) they are among the most potent pyrogens known, (*b*) they are all capable of inducing a highly lethal toxic shock syndrome, and (*c*) they share a typical three-dimensional structure consisting of two domains, termed large and small. The small domain is a β-barrel made up of two β-sheets, whereas the large domain contains a β-grasp motif, an α-helix packed against a mixed β-sheet that connects the peripheral strands (9–16). Nevertheless, each of these molecules has unique biological properties and stimulates the proliferation of T cells with different Vβ regions. Among their biological effects, the staphylococcal enterotoxins are characterized by their ability to induce emesis and diarrhea, whereas TSST-1 lacks emetic activity. The streptococcal toxins do not cause enteric problems but they are associated with cardiotoxicity. The level of sequence homology between the pyrogenic toxins varies widely, and they can be divided into groups based on sequence similarities. The highest degree of homology is achieved by SEA, SED, and SEE (between 53–81%), followed by the group of SEB, the SECs, SPEA, and SSA, with 50–66% of sequence homology. All the rest, including SPEB, SPEC, SPEF, and TSST-1, have poor or no homology to any other toxin, or to each other.

Bacterial SAGs that do not belong to the pyrogenic toxin family include the staphylococcal exfoliative toxins (ET) A and B (17, 18), *Mycoplasma arthritidis* mitogen (MAM) (19), and *Yersinia pseudotuberculosis* mitogen (20, 21).

Among superantigenic proteins of viral origin, only mouse mammary tumor virus (MMTV)-encoded SAGs have been defined in detail (22). It has been demonstrated that mouse Mls endogenous SAGs are encoded by MMTV proviral DNA that has been integrated into the germline, demonstrating a link between endogenous SAGs and infectious agents. Other reports have shown superantigenic activity by the rabies virus nucleocapsid protein (23) and by two human tumor viruses, cytomegalovirus (24) and Epstein-Barr virus (25). Recently, the envelope gene of an endogenous human retrovirus isolated from pancreatic islets was shown to encode an MHC class II–dependent SAG specific for Vβ7 (26).

The past four years have witnessed a remarkable series of advances in knowledge of the three-dimensional structure of TCRs (27–32) and of their complexes with peptide/MHC (33–35) and SAGs (36, 37). In this review, we focus on TCR-SAG interactions and describe current understanding of the structural basis of T cell activation by SAGs. After giving an overview of the biological effects of bacterial and viral SAGs, we discuss the affinity and kinetics of TCR and MHC binding to these molecules. We then describe the three-dimensional structures of MHC-SAG and TCR β chain-SAG complexes. These structures, along with those of TCR-peptide/MHC complexes, reveal how SAGs circumvent the normal mechanism for T cell activation by peptide/MHC and how they stimulate T cells expressing TCR β chains from a number of different families, resulting in polyclonal T cell activation. Finally, we discuss the structural basis for the specificity of different SAGs for particular TCR β chains and for the observed influence of the TCR α chain on SAG reactivity.

BIOLOGICAL EFFECTS OF SUPERANTIGENS

T Cell Anergy and Deletion

The specificity of interaction of SAGs with the Vβ domain of the TCR has provided a unique opportunity to examine the fate of reactive T cells in vivo independently of functional assays. Such studies have revealed that responding T cells can proliferate, become nonresponsive (anergy), or even die (deletion) (38, 39). In the in vivo recognition of endogenous SAGs, intrathymic deletion in Vβ-specific subsets occurs at the double-positive ($CD4^+$, $CD8^+$) stage of development, and deletion is correspondingly apparent in both the mature $CD4^+$ and $CD8^+$ subsets (40–42). In the case of exogenous SAGs, an early report showed that mice injected from birth with SEB virtually lack V$\beta3^+$ and V$\beta8^+$ mature thymocytes, giving the first formal demonstration that clonal deletion can accompany induced tolerance to a foreign antigen (43). Subsequent studies confirmed this report and showed that in adult mice, SEB-specific mature T cells can, after an initial expansion, be rendered anergic in both in vivo and in vitro

models (44, 45). Moreover, SEB-induced death of Vβ8$^+$ cells is independent of an intact thymus, because it also occurs in adult thymectomized animals (46).

The presence of a SAG in the MMTV genome can guarantee the existence of actively dividing populations of T and B cells through the ability of the SAG to stimulate T cells, and, thus, let the virus complete its replication cycle (22). This was confirmed using mice transgenic for the MMTV (C3H) *sag* gene (47). The SAG-mediated deletion of Vβ14$^+$ T cells during early life conferred resistance to infection to these mice. Similar results were observed for a different exogenous MMTV, called SW, where the corresponding SAG stimulates Vβ6$^+$ cells (48). Because MMTV infection occurs during the shaping of the immune repertoire in neonatal life and because infection is persistent, there is a gradual deletion of SAG-reactive T cells (49). Finally, there is no evidence for a SAG-independent pathway of MMTV transmission, and only MMTV with functional *sag* genes can be transmitted through milk (50, 51). Once the SAG is stably integrated into the mouse genome, it can be inherited by successive generations. When expressed endogenously, it causes deletion of cognate T cells and prevents a reinfection with the same strain of virus that produces the SAG (47, 48).

Toxic Shock Syndrome and Food Poisoning

Toxic shock syndrome (TSS) is an acute, life-threatening intoxication characterized by high fever, hypotension, rash, multiorgan dysfunction, and cutaneous desquamation that is caused by staphylococcal or streptococcal pyrogenic toxins (6, 52–54). The interaction of the pyrogenic toxins with TCR and MHC activates both the T cell, for secretion of TNFβ, IL-2, and γ interferon, and the APC, for secretion of TNFα and IL-1. The resulting massive cytokine release is believed to be responsible for capillary leak and hypotension, and it is also likely to cause the erythematous rash in TSS patients (52, 54).

Staphylococcal enterotoxins are among the most common causes of food poisoning in humans. It has been suggested that the enterotoxic effects are directly related to their superantigenic activity, i.e. dependent on T cell stimulation and probably caused by massive cytokine release (3, 6). However, some evidence suggests that the emetic and T cell proliferative activities of the toxins may be distinct (3, 55–57). In fact, the induction of emesis has been attributed to leukotriene or histamine release (58). It has been shown that SEB and SEA can rapidly cross an epithelial membrane in intact, fully functional form, thus gaining access to T cells. On the contrary, TSST-1, which lacks emetic activity, although able to transcytose epithelium, may be more easily destroyed by digestive enzymes in the stomach and intestine (59). Thus, the ability to cause enterotoxicity may be related to the resistance to digestion of the enterotoxins.

Autoimmune Diseases

In autoimmune diseases, a breakdown of self-tolerance leads to the generation of an immune response against a specific target antigen or antigens. A large body of clinical and epidemiological evidence indicates that infections are important in the induction of autoimmune disorders such as autoimmune myocarditis (60) and insulin-dependent diabetes mellitus (61). One mechanism by which this has long been thought to occur is through the activation of autoreactive T cells by epitopes on microbial antigens that are cross-reactive with antigens on target organs (62). For example, a number of viral and bacterial peptides have been identified that efficiently activate myelin basic protein (MBP)-specific T cell clones from multiple sclerosis (MS) patients (63, 64). More recently, it has been proposed that SAGs derived from bacteria, mycoplasma, or viruses may initiate autoimmune disease by activating specific anti-self T cell clones (3, 65). Indeed, microbial SAGs have been shown to trigger clinical relapses of autoimmune disease in several animal models, as discussed below. The expansion of selected Vβ families in the affected organs or peripheral blood of certain individuals with autoimmune disease has also been documented (3, 65). However, it is a common observation that different TCR repertoire studies of the same disease can provide different results (66). Even when it is unlikely that SAGs by themselves initiate an autoimmune disease (65), they may modulate disease pathogenesis. In susceptible individuals, the activation of autoreactive T cells is a necessary, but not sufficient, condition for the development of an autoimmune disease. A sufficient degree of clonal expansion of autoreactive T cells may be a major limiting factor, and SAGs may induce such an expansion. Alternatively, the activation of B lymphocytes and other APC through the SAG bridge may lead to the secretion of autoantibodies and interleukins that contribute to inflammation.

Evidence for an autoimmune origin of MS comes from (*a*) the presence of $CD4^+$ T cells and cells expressing MHC class II molecules in inflamed tissues (67), (*b*) the finding that MS is associated with certain MHC class II alleles (68), and (*c*) the demonstration that MBP-specific T cells are clonally expanded in MS patients (69–72). In experimental autoimmune encephalomyelitis (EAE), a model for MS, administration of SEB to PL/J mice following immunization with a peptide derived from MBP (Ac1-11) was found to induce paralysis in mice with subclinical disease and to trigger relapses in mice that are in remission following an initial episode of paralysis (73–75). It was shown that these effects are the direct result of stimulation by SEB of Vβ8-expressing encephalitogenic T cells specific for MBP Ac1-11.

An analysis of the TCR β chain repertoire of synovial T cells from rheumatoid arthritis (RA) patients revealed a selective expansion of Vβ14-bearing T cells compared with the levels in the peripheral blood of the same

individuals (76). A mechanism for the pathogenesis of RA was proposed in which a microbial SAG activates disease-mediating Vβ14$^+$ T cells and allows these activated cells to enter the synovial tissue, where they persist because of reactivation by autoantigens. In collagen II–induced arthritis (CIA), a model for RA, mice are immunized with native porcine type II collagen and develop joint swelling. It has been demonstrated that T cells expressing Vβ8 are important in the development of CIA (77–80) and that administration of SEB 10 days prior to a collagen II challenge protects mice from CIA (81). In both EAE and CIA, the response to self-antigens is controlled by a potent regulatory T cell circuitry based on recognition of different determinants derived from the TCR Vβ8.2 chain (81–83). The SAG MAM, which derives from a naturally occurring mouse arthritogenic mycoplasma, activates Vβ8$^+$ T cells. Administration of MAM has been shown to markedly exacerbate arthritis in mice that were convalescent from CIA, or to trigger arthritis in animals previously immunized with collagen II but that had failed to develop clinical disease (19).

Insulin-dependent diabetes mellitus (IDDM) is an autoimmune disease affecting pancreatic β cells that secrete insulin. A relationship between viral infections and the development of IDDM has been long suspected (84). An analysis of pancreatic islet–infiltrating T cells from patients with IDDM revealed preferential expression of the Vβ7 gene segment, but no selection for particular Vα segments or Vβ-D-Jβ junctional sequences (85, 86). This led to the proposal that a SAG associated with pancreatic islets may be involved in the pathogenesis of IDDM. This putative SAG was recently identified by Conrad et al (26), who isolated a novel human endogenous retrovirus from supernatants of IDDM islets and showed that the envelope gene encodes an MHC class II–dependent SAG specific for Vβ7.

Kawasaki disease (KD) is an acute febrile illness with symptoms similar to toxic shock syndrome. Several studies have revealed a significantly elevated level of circulating Vβ2$^+$ and, to a lesser extent, Vβ8.1$^+$ T cells in patients with acute KD, compared with control populations (87–90). Sequencing of these β chains revealed extensive junctional region diversity, which suggests activation by SAG and not a specific disease-associated antigen. Bacteria-producing toxins that activate Vβ2$^+$ T cells (TSST-1 and SPEB/SPEC) were isolated from 13 out of 16 KD patients but only 1 out of 15 in the control group (91). Nevertheless, other groups were not able to document the expansion of any Vβ family during the acute phase of KD (92, 93). Differences in population studied, method and time of collecting samples, and techniques used could potentially explain the differences in results. Alternatively, the expansion of selected Vβ families may not be related to the pathogenesis of the disease (94).

Skin Diseases

The staphylococcal toxins ETA and ETB induce the symptoms associated with staphylococcal scalded skin syndrome, characterized by a specific intraepidermal separation of layers of the skin (95). X-ray crystallographic studies of ETA have shown that its overall structure is similar to that of the chymotrypsin-like serine protease family of enzymes (17, 18). The catalytic triad includes the residue Ser195, which when mutated to cysteine abolishes the characteristic separation of epidermal layers, although the ability to induce T cell proliferation is not altered (17, 96). These findings suggest that skin separation is the result of a specific proteolysis by ETA, and not related to its superantigenic activity; the latter is probably involved in the edema or redness associated with scalded skin syndrome.

Psoriasis is a disease characterized by increased proliferation of epidermal cells associated with an inflammatory component. Patients with acute guttate psoriasis often have flares of psoriasis following streptococcal infections (97). Histological examination of early skin lesions shows that infiltration of lymphocytes and macrophages into the skin precedes the characteristic epidermal proliferation of psoriasis. The predominant distribution of Vβ2-, Vβ3-, and Vβ5-bearing T cells in lesional skin of acute guttate psoriasis has been described (98–100). However, there are conflicting reports about the restricted T cell receptor repertoire in chronic psoriasis (98, 101), and no increase in SAG-producing *Staphylococcus aureus* has been seen in chronic psoriatic patients (102). It is unlikely, then, that SAGs are essential to the continuance of psoriasis, although they may be exacerbating factors or triggers for the disease.

Atopic dermatitis is a chronic pruritic inflammation of the skin characterized by local infiltration of monocytes and lymphocytes, mast cell degranulation, and immediate and delayed hypersensitivity (103). There are numerous reports that *S. aureus* can exacerbate this disease, and *S. aureus* was isolated from the affected skin of more than 90% of patients (104). More than half of the patients had *S. aureus* that secreted SEA, SEB, and TSST-1 (105). Sera from 57% of atopic dermatitis patients contained immunoglobulin E specific for one or more of these SAGs. Thus, epicutaneous superantigenic toxins might induce specific immunoglobulin E in atopic dermatitis patients, as well as mast cell degranulation.

AFFINITY AND KINETICS OF TCR BINDING TO SUPERANTIGENS

Gascoigne & Ames first demonstrated direct binding of a soluble TCR β chain (mouse Vβ3) to SEA presented by MHC class II molecules on cells (106).

However, the affinity was too low to be measured in their cell-binding assay. More recently, the development of surface plasmon resonance techniques for detecting macromolecular interactions (107) has permitted the precise measurement of kinetic and affinity constants for TCR binding to SAGs, as well as to peptide/MHC complexes (108). By this method, a soluble human TCR (Vβ3.1) was found to bind immobilized SEB in the absence of MHC class II molecules with a dissociation constant (K_D) of 0.8 μM; the on-rate (k_{on}) of the interaction was 1.3×10^4 M^{-1} s^{-1} and the off-rate (k_{off}) 1.1×10^{-2} s^{-1} (109). Specific binding of soluble 14.3.d TCR β chain (mouse Vβ8.2) was demonstrated to SEB, SEC1, SEC2, SEC3, and SPEA, consistent with the known proliferative effects of these SAGs on T cells expressing Vβ8.2 (110). In contrast, SEA, which does not stimulate Vβ8.2-bearing cells, did not bind the recombinant β chain. Affinities ranged from 3 μM for SEC3 to 140 μM for SEB; k_{on} and k_{off} were too fast to be accurately measured, but were estimated at $>10^5$ M^{-1} s^{-1} and >0.1 s^{-1}, respectively (110, 111). The unpaired β chain was shown to fully retain the SAG-binding activity of the assembled 14.3.d $\alpha\beta$ TCR heterodimer (110). A K_D of 1.1 μM was measured for the binding of SEC2 to the mouse D10 TCR (Vβ8.2), with a k_{on} of 1.7×10^4 M^{-1} s^{-1} and a k_{off} of 1.9×10^{-2} s^{-1} (112). These values closely resemble those for the interaction of D10 TCR with its cognate peptide/MHC class II ligand, which has a K_D of 2.1 μM and a k_{on} and k_{off} of 1.0×10^4 M^{-1} s^{-1} and 2.2×10^{-2} s^{-1}, respectively (112).

In each of the above examples, TCR-SAG binding is characterized by low affinities ($>10^{-6}$ M) and very fast k_{on} and k_{off} ($>10^4$ M^{-1} s^{-1} and $>10^{-2}$ s^{-1}, respectively). It is noteworthy that low affinities and rapid dissociation kinetics have also been reported for the interaction of other T cell surface glycoproteins with their ligands, such as the adhesion molecule CD2 with CD48 (113, 114). In particular, the affinities of TCR-SAG interactions (10^{-4}–10^{-6} M) are remarkably similar to those reported for the binding of TCRs to specific peptide/MHC complexes (10^{-4}–10^{-7} M) (115–117) and are much weaker than those of antigen-antibody reactions (typically 10^{-8}–10^{-11} M). In the case of adhesion molecules, fast dissociation rates may facilitate deadhesion, a requirement for cell motility (113). In the case of TCRs, rapid off-rates may permit a single peptide/MHC complex to sequentially bind and trigger a large number of TCRs (up to 200), as proposed in the serial triggering (118, 119) and kinetic proofreading (120) models of T cell activation, until a certain activation threshold is reached. The finding that the binding of bacterial SAGs to the TCR is characterized by low affinities and fast dissociation kinetics suggests that SAGs mimic the interaction of peptide/MHC complexes with the TCR in terms of affinity and kinetics and that some form of serial engagement may also operate in T cell activation by SAGs (111, 119, 121).

The relationship between the affinity of SAGs for TCR and MHC and their ability to activate T cells has been investigated using site-directed mutants of

SEC3 and SEB (111). In order to mimic normal physiological conditions as closely as possible, resting lymph node T cells bearing the 14.3.d TCR from RAG-$2^{-/-}$ TCR transgenic mice were used to measure the stimulatory effects of mutant SAGs on BALB/c spleen cells expressing I-E^d, or on MHC class II–negative mouse fibroblasts transfected with a gene encoding human leukocyte antigen (HLA)-DR1. A clear and simple relationship was observed between the affinity of SAGs for the TCR and their mitogenic potency: the tighter the binding of a particular mutant of SEC3 or SEB to the TCR β chain, the greater its ability to stimulate T cells. The affinities of the SAGs tested ranged from 3.5 μM to >250 μM. However, an apparent exception to this simple affinity-activity rule was the finding that SEB stimulated transgenic T cells about 10-fold better than did SEC3, even though the affinity of SEB for the TCR β chain (140 μM) is much lower than that of SEC3 (111). To determine whether the surprisingly strong mitogenic potency of SEB relative to SEC3 could be attributed to tighter binding to MHC class II on APC, the binding of SEB and SEC3 to soluble recombinant HLA-DR1 was measured by sedimentation equilibrium: Whereas SEB bound to DR1 with a K_D of 14 μM, the corresponding value for SEC3 was 48 μM. Therefore, the unexpectedly high mitogenic potency of SEB relative to SEC3 can be explained by the stronger binding of SEB to MHC class II. This indicates that mitogenic potency is the result of an interplay between TCR-SAG and SAG-MHC interactions, such that a relatively small (threefold) increase in the affinity of a SAG for MHC can overcome a large (35-fold) decrease in the affinity of a SAG for the TCR.

With the apparent affinities of SAGs for both TCR and MHC class II molecules in the micromolar range, nearly all SAG molecules will be unbound at physiological SAG concentrations (10^{-12}–10^{-15} M) (121). Under these conditions, it is difficult to understand how a SAG can effectively cross-link the T cell and APC. The problem is seemingly less severe for peptide/MHC because the peptide is, in effect, irreversibly bound to MHC. One possible explanation for the ability of SAGs to trigger T cells at concentrations orders of magnitude less than their K_Ds is that accessory molecules such as CD4 help stabilize the TCR-SAG-MHC complex sufficiently for activation to occur. Another is that the overall stability of the TCR-SAG-MHC complex is considerably greater than would be expected from considering the TCR-SAG and SAG-MHC interactions independently. That is, the binding of SAGs may be a cooperative process in which the SAG-MHC complex binds the TCR with greater affinity than does the SAG alone. This hypothesis is supported by the finding that the affinity of SEB for a soluble human TCR was significantly enhanced by the addition of soluble HLA-DR1 (109). The potential role of the TCR α chain in stabilizing the TCR-SAG-MHC complex is discussed in a later section.

STRUCTURE OF SUPERANTIGEN–MHC CLASS II COMPLEXES

The three-dimensional structures of three SAG-MHC class II complexes have been determined by Wiley and colleagues: (*a*) the complex between SEB and HLA-DR1 to 2.7-Å resolution (122), (*b*) the complex between SEB and HLA-DR4 to 2.5-Å resolution (123), and (*c*) the complex between TSST-1 and HLA-DR1 to 3.5-Å resolution (124). In the SEB–HLA-DR1 complex [Figure 1*A* (see color plates)], SEB binds to the α1 domain of DR1, contacting residues from the first and third turns of the β-sheet and from the N-terminal portion of the α-helix (122). The binding of SEB to DR4 is similar (123). The ability of SEB to bind many different DR alleles can therefore be explained by its exclusive interaction with the DR1 α chain, which is conserved in all DR molecules. Residues of SEB in contact with DR1 derive mainly from the small domain of the SAG, although several residues from the large domain also contact the DR α chain. SEB binds away from the peptide-binding groove of DR1 and does not contact the bound peptide. The affinity of SEB for DR1 was reported as approximately 0.5 μM in a cell-binding assay (125) and as 14 μM using soluble DR1 (111).

Although the TSST-1 binding site on HLA-DR1 overlaps that of SEB, the two SAGs bind differently (124). Whereas SEB binds primarily off one edge of the peptide-binding groove (Figure 1*A*), TSST-1 extends over nearly half the binding groove and contacts the α-helix of the α1 domain of DR1, the bound peptide, and part of the α-helix of the β1 domain of DR1 (Figure 1*B*). This binding mode suggests that the interaction of TSST-1 with MHC class II molecules may be partially peptide dependent. In agreement with the crystal structure, certain peptides were found to promote the presentation of TSST-1 by I-A^b up to 5000-fold (126). In contast, the binding of SEB to I-A^b and I-E^{dk} is peptide independent (126, 127).

Although no crystal structures have been reported for SEA complexed with MHC class II molecules, mutagenesis and binding studies have demonstrated that SEA possesses two distinct, yet cooperative, binding sites for class II molecules: (*a*) a low-affinity site ($K_D = 10^{-5}$ M) to the DR1 α chain analogous to the DR1-binding site of SEB, and (*b*) a Zn^{2+}-dependent, high-affinity site ($K_D = 10^{-7}$ M) to the polymorphic DR1 β chain (127–129). Binding of one SEA molecule to the DR1 β chain enhances the binding of a second SEA molecule to the DR1 α chain (128, 129). Surprisingly, mutations in the Zn^{2+}-dependent site completely abolish SEA activity, even though it can still bind the DR1 α chain through its low-affinity SEB-like site. This suggests that MHC cross-linking on the surface of APC may be an essential feature of SEA function. This conclusion is supported by the demonstration that SEA_2-DR1

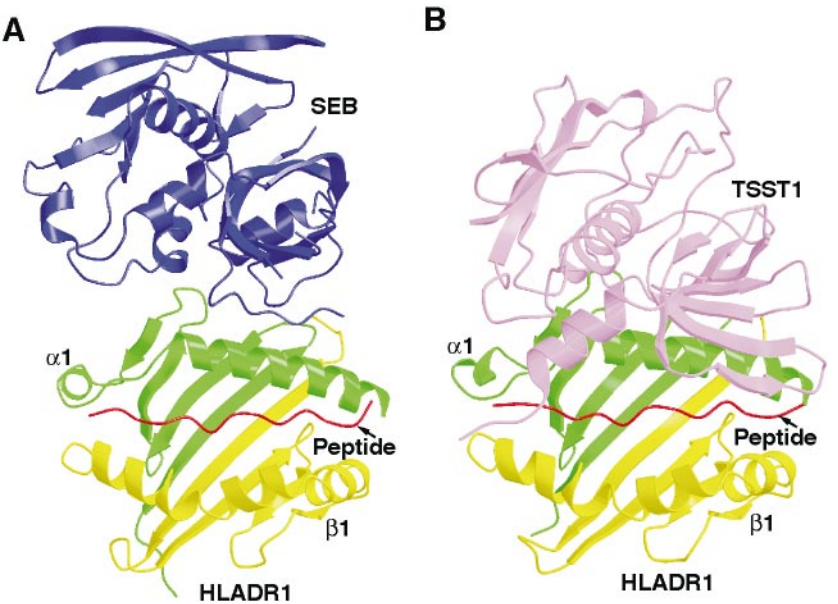

Figure 1 Three-dimensional structures of the complexes between HLA-DR1 and SEB and between HLA-DR1 and TSST-1. (*A*) Ribbons diagram of the SEB-HLA-Dr1 complex (122). (*B*) Ribbons diagram of the TSST-HLA-DR-1 complex (124). Colors are as follows: SEB (*blue*), TSST-1 (*pink*), DR1 α1 domain (*green*), DR1 β domain (*yellow*), and peptide (*red*).

trimers exist in solution (130), as well as by the finding that SEA mediates signaling through the APC by direct cross-linking of DR1 molecules (131, 132). The high sequence identity between SEE and SEA (see Figure 3*A*) suggests that they may bind class II molecules similarly. Two additional SAGs have been described that cross-link class II molecules, but by different mechanisms than SEA. The crystal structure of SED shows that this SAG forms dimers in the presence of Zn^{2+} by coordinating two Zn^{2+} ions between the large domains of two SED molecules (15). Binding to MHC class II molecules is believed to occur through the small domain to the class II α chain in a manner similar to SEB, resulting in a tetrameric class II α–SED-SED–class II α complex on the APC. The three-dimensional structure of SPEC reveals that the class II α chain-binding site on the small domain has been replaced by SPEC dimer interface (16). Instead, SPEC binds only to the class II β chain. This could potentially lead to the formation of class II β–SPEC-SPEC–class II β tetramers. Dimeric SAGs like SED and SPEC may facilitate TCR dimerization and subsequent T cell triggering.

Endogenous SAGs encoded by MMTV can be efficiently presented to T cells only by B cells, through interaction with MHC class II molecules (22). Although direct binding has been demonstrated between recombinant forms of MMTV SAGs and MHC class II molecules (133, 134), the interaction remains poorly understood. I-E molecules are the best presenters for all the described MMTV SAGs (135). In addition, C57BL mice that lack I-E molecule, and thus are not able to present SAG to T cells, are resistant to milk-borne MMTV (C3H) (136). Analysis of class II mutants that lost the ability to present bacterial SAGs revealed that bacterial SAGs have different binding requirements than do MMTV SAGs (137). Another study showed, however, an overlap in at least one binding site for MMTV and SEA on the MHC molecule (138). Recently it was shown that N-linked glycosylation is required for effective B cell presentation of MMTV SAGs to T cells (139).

STRUCTURE OF TCR β CHAIN–SUPERANTIGEN COMPLEXES

The three-dimensional structures of several TCR β chain–SAG complexes have been determined to date, each involving the VβCβ chain of the mouse 14.3.d TCR specific for a hemagglutinin peptide of influenza virus bound by the I-E^d class II molecule: (*a*) the complex between the β chain and SEC2 to 3.5-Å resolution (36), (*b*) the complex with SEC3 to 3.5-Å resolution (36), (*c*) the complex with SEB to 2.4-Å resolution (37), and (*d*) the complex with a mutant of SEB in which valine at position 26 is replaced by tyrosine (SEB V26Y) to 2.6-Å resolution (37). The SEB V26Y mutant was designed on the

basis of the structure of the TCR β–SEC3 complex to bind the β chain more tightly than wild-type SEB: Its K_D is 12 μM, approximately 12 times lower than that of SEB ($K_D = 140\ \mu$M), but still four times higher than that of SEC3 ($K_D = 3\ \mu$M) (111). The mutant is fourfold more active in T cell proliferation assays than is wild-type SEB, consistent with its enhanced affinity.

The crystal structures of the TCR β–SEC2/3 complexes identified the regions of the β chain recognized by SEC and showed how SAGs circumvent the normal mechanism for T cell activation by specific peptide/MHC complexes. However, the moderate resolution of these structures (3.5 Å) precluded a detailed analysis of the interface between the two proteins in terms of hydrogen bonds, van der Waals interactions, and solvent structure. To achieve a more complete description of a β-SAG interface, as well as to assess whether conformational changes occur in either or both proteins upon complex formation, the structures of the complexes between the 14.3.d β chain and SEB and SEB V26Y were determined to high resolution (37). These structures, along with those of $\alpha\beta$ TCR heterodimers (29–31) and TCR-peptide/MHC complexes (33–35), can account for the specificity of different SAGs for particular β chains and for the influence of the TCR β chain on SAG reactivity (5, 140–142).

Overall Structure of the TCR β–SEB and TCR β–SEC Complexes

The overall structure of the β-SEB complex is shown in Figure 2*A* (see color plates). The complex is formed through contacts between the Vβ domain and the small and large domains of SEB. The complementarity-determining region (CDR)2 of the TCR β chain and, to lesser extents, hypervariable region (HV)4 and framework regions (FR)2 and -3 bind in the cleft between the two domains of the SAG (37). This binding mode is similar to that observed in the β-SEC2 and β-SEC3 complexes (36), but with several differences, as discussed below. SEC2 and SEC3 bind identically to the 14.3.d β chain, and none of the four amino acid differences between SEC2 and SEC3 is located in the complex interface. This is reflected in the K_Ds of the two SAGs, which are both approximately 3 μM. The TCR-binding sites of SEC3 and SEB, in contrast, differ at positions 20, 26, and 91; these differences presumably account for the 45-fold weaker affinity of SEB for the 14.3.d β chain (111).

The solvent-excluded surface area for the β-SEB complex is 1343 Å^2 (685 Å^2 from Vβ and 658 Å^2 from SEB); the buried surface area for the β-SEC3 complex is similar (1300 Å^2). These values are within the range observed for antigen-antibody complexes (143) but somewhat smaller than the approximately 1800 Å^2 of buried surface in TCR-peptide/MHC complexes (33–35). As shown in Figure 2*A*, the TCR-binding site of SEB is adjacent to, but distinct from, the MHC-binding site of this SAG (122, 123). This spatial proximity

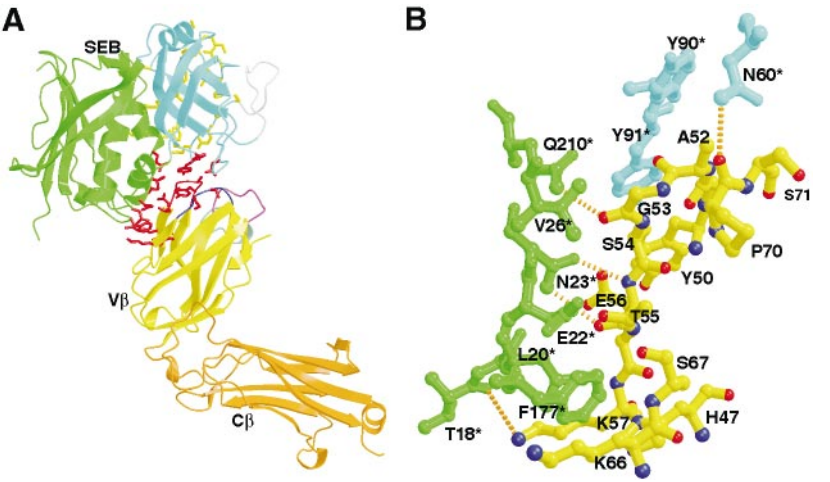

Figure 2 TCR β-SEB complex. (*A*) Ribbons diagram of the VβCβ-SEB complex (37). Colors are as follows: Vβ (*yellow*), CDR1 (*pink*), CDR2 (*red*), CDR3 (*gray*), HV4 (*blue*), Cβ (*brown*), SEB large domain (*green*), and SEB small domain (*blue*). Residues of Vβ and SEB involved in interactions in the TCR-SAG interface are red. Residues of SEB in contact with MHC in the structure of the SEB-HLA-DR1 complex (122) are yellow. The SEB disulfide loop (*light gray*), which is not visible in the electron density map of the β-SEB complex, was modeled according to the uncomplexed SEB crystal structure (9). (*B*) Interactions in the β-SEB interface. View is the same as in *panel A*. Vβ atoms are colored accordingly to atom type: carbon, nitrogen and oxygen atoms are *yellow, blue*, and *red*, respectively. SEB atoms are colored *green* (large domain) and *blue* (small domain). SEB residues are indicated with asterisks. Hydrogen bonds are *dotted brown lines*.

suggests that the two binding sites may not be completely independent; that is, the affinity of the TCR for SEB alone may be lower (or higher) than its affinity for SEB bound to MHC class II molecules.

Structure of the β-SEB and β-SEC Interfaces

The Vβ residues in contact with SEB are as follows: His47 of FR2; Tyr50, Ala52, Gly53, Ser54, and Thr55 of CDR2; Glu56, Lys57, Tyr65, Lys66, and Ala67 of FR3; and Pro70 and Ser71 of HV4 (Table 1). The FR2, CDR2, FR3, and HV4 regions contribute 7%, 50%, 34%, and 9%, respectively, of the total contacts to SEB. The crystal structure therefore readily accounts for mutational and genetic evidence implicating Vβ CDR2 and HV4 in SAG recognition (3). In the β-SEC3 complex (36), the Vβ residues in contact with the SAG are as follows: Tyr50, Ala52, Gly53, Ser54, and Thr55 of CDR2; Glu56, Lys57, and Lys66 of FR3; and Pro70 and Ser71 of HV4 (Table 1). The CDR2, FR3, and HV4 regions contribute 63%, 32%, and 7%, respectively, of the total contacts to SEC3. Thus, although there are several differences in contacting residues in the two complexes (e.g. Vβ FR2 His47, which contacts SEB but not SEC3, and Vβ CDR2 Gly51, which contacts SEC3 but not SEB), CDR2 and FR3 account for the majority of interactions with the SAG in both complexes, with HV4 playing only a secondary role. The binding sites on the TCR for SAG and peptide/MHC class I molecules only partially overlap. As shown in Table 1, only Vβ residues Tyr50, Ala52, Thr55, and Glu56 contact both SEB and peptide/MHC in the 2C TCR-dEV8/H-2K^b complex (34).

The SAG residues in contact with Vβ are as follows: Asn60, Tyr90, and Tyr91 (Val91 in SEC3) of the small domain; and Thr18, Gly19, Leu20 (Thr20 in SEC3), Glu22 (in β-SEB only), Asn23, Tyr26 (in β-SEC3 and β-SEB V26Y only), Phe177 (Phe176 in SEB), and Glu210 of the large domain (Table 1). Residues Asn23, Asn60, and Tyr90 are strictly conserved among bacterial SAGs reactive with mouse Vβ8.2, including SEC1–3 and SPEA, and have been shown to constitute energetic hot spots for binding the 14.3.d β chain (111) (Figure 3*A*, see color).

The structures of the β-SEB and β-SEC complexes enable us to understand how SEB and SEC, which have nearly identical Vβ specificities, can each stimulate T cells expressing Vβ domains from a number of different families (3). As shown in Figure 2*B*, all the hydrogen bonds between SEB and Vβ are formed between SEB side-chain atoms and Vβ main-chain atoms, except for a hydrogen bond between the main-chain oxygen of SEB Thr18 and the side chain of Vβ Lys57 (SEB Thr18 O-Nζ Lys57 Vβ). Four of the main-chain–side-chain hydrogen bonds in the β-SEB complex are also present in the β-SEC3 complex: Vβ Gly53 O-Nε2 Gln210 SEB, Vβ Thr55 N-Oδ1 Asn23 SEB, Vβ Thr55 O-Nδ2 Asn23 SEB, and Vβ Pro70 O-Nδ2 Asn60 SEB (Table 1).

A

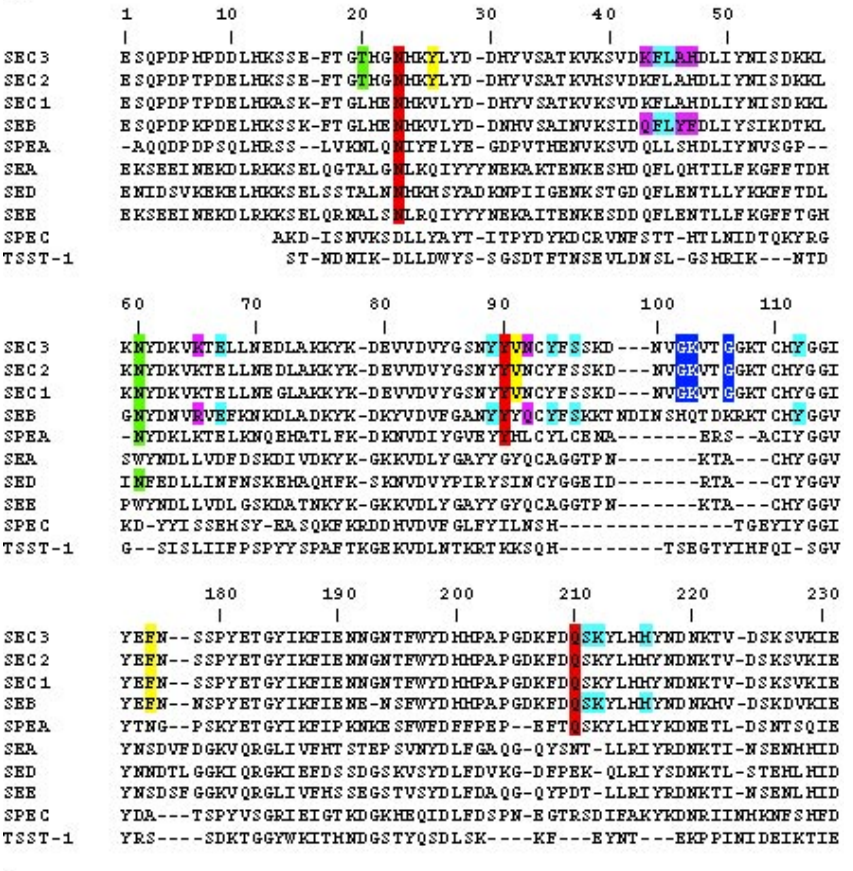

B

	47	50	51	52	53	54	55	56	57	65	66	67	70	71
mVβ8.2	H	Y	G	A	G	S	T	E	K	Y	K	A	P	S
mVβ3	I	Q	N	Q	E	V	L	Q	Q	F	S	A	P	S
mVβ7	Y	Y	D	V	D	S	N	S	E	Y	R	V	K	K
mVβ10	F	N	N	K	Q	L	I	V	N	F	S	P	S	S
mVβ17	I	R	N	E	E	I	H	E	Q	F	S	A	S	S
hVβ3	Y	Y	D	V	K	H	K	E	K	Y	S	V	E	K
hVβ5	F	F	S	E	T	Q	R	N	K	F	S	G	F	S
hVβ12	H	Y	G	V	K	D	T	D	K	Y	S	V	S	K
hVβ13.2	H	V	G	E	G	T	T	A	K	Y	N	V	L	K
hVβ14	Y	H	N	V	E	V	T	D	K	Y	K	V	K	E
hVβ15	Y	F	D	V	K	D	I	N	K	Y	S	V	Q	A
hVβ17	Y	Q	I	V	N	D	F	Q	K	Y	S	V	E	K
hVβ20	F	V	G	I	G	Q	I	S	S	L	S	A	P	Q

Figure 3 Residues defining the interaction of bacterial SAGs with TCR β chains. (*A*) Sequence alignment of bacterial SAGs (SEB, SEC1-3, SPEA, SEA, SED, SEE, SPEC, TSST-1) based on structural information. The α-carbon skeletons were first optimally superposed. Sequences were then manually adjusted to minimize the number of gaps while respecting the structural similarity. Residues 116-173 and 232-239 are not shown. SEC3 residues in contact with the TCR β chain are boxed in colors according to the loss of binding free energy ($\Delta\Delta$G) upon alanine substitution: (*red*) $>$2.5 kcal/mol; (*yellow*) 1.5-2.5 kcal.mol; (*green*) 0.5-1.5 kcal/mol; (*blue*) $<$0.5 kcal/mol (111). The homologous residues in the other SAGs are only boxed in color if they are identical with those in SEC3. SEB residues contacting MHC in the crystal structure of the SEB-HLA-DR1 complex (122), and the corresponding residues of SEC3, are boxed in *cyan* if identical in SEB and SEC3 and in *magenta* if different. (*B*) Sequence alignment of selected mouse (m) and human (h) TCR β chains reactive with SEB or SEC(3). Only SAG-containing residues are shown.

Table 1 Contacts between the 14.3.d TCR β chain and staphylococcal SAGs[a]

Hydrogen bonds					
β		SEB[b]		SEC3[b]	
G53	O	Q210	Nε2	Q210	Nε2
T55[c]	N	N23	Oδ1	N23	Oδ1
	O		Nδ2		Nδ2
	O			T20	Oγ1
K57	Nζ	T18	O		
P70	O	N60	Nδ2	N60	Nδ2

Van der Waals contacts[d]				
β	SEB	No. of contacts	SEC3	No. of contacts
H47	L20	1		
	F177	4		
Y50[c]	Y91	10	V91	1
G51			V91	4
A52[c]	Y90	4	Y90	5
G53	N23	1	N23	1
			Y26	7
			Q210	4
S54	N23	2	N23	5
			V91	1
T55[c]	L20	4	T20	2
	N23	2	N23	4
	E22	2		
	F177	1		
E56[c]	L20	1	T20	1
	N23	1		
K57	G19	3	G19	4
	L20	2	T20	4
Y65	F177	1		
K66	F177	6	F176	7
A67	F177	4	F176	3
P70	N60	2	L58	1
S71	N60	2	N60	1

[a] TCR, T cell receptor; SAG, superantigen; SE, staphylococcal enterotoxin; MHC, major histocompatibility complex.

[b] Data for the β-SEB and β-SEC3 complexes are from References 37 and 36, respectively.

[c] Vβ residues in contact with peptide/MHC in the 2C TCR-dEV8/H-2K^b complex (34).

[d] Van der Waals contacts <4.0 Å.

The importance of these conserved interactions to complex stabilization is demonstrated by the finding that SEC3 mutants Asn23 → Ala and Gln210 → Ala bind the TCR β chain 70-fold less tightly than does the wild-type SAG, whereas SEC3 Asn60 → Ala binds 16-fold less tightly (111). A recognition mechanism involving a major role for main-chain hydrogen bonds can be highly sequence independent, enabling SEB or SEC to recognize virtually any Vβ domain in which the positions of the relevant main-chain atoms are close to those of mouse Vβ8.2; a similar binding mode has been described for peptide/MHC complexes (144, 145). A sequence alignment of mouse and human Vβ families reactive with SEB or SEC illustrates the diversity of amino acids that can be accommodated at Vβ-contacting positions (Figure 3*B*).

Four water molecules were found to form hydrogen bonds bridging Vβ and SEB: Vβ Ala67 O-H_2O-Oε2 Glu22 SEB, Vβ Tyr50 O-H_2O-O Tyr91 SEB, Vβ Tyr65 O-H_2O-Nδ2 Asn178 SEB, and Vβ Lys66 Nζ-H_2O-N Phe177 SEB. Bound water molecules have also been observed in the combining site of antibodies, where they act to increase complementarity in the interface with antigen (146–148).

There are no direct contacts between SEB or SEC and Vβ CDR3, which folds away from the SAG (Figure 2*A*, Table 1); this is consistent with the finding that bacterial and viral SAGs stimulate T cells expressing particular Vβ elements without obvious selection for Vβ CDR3 length or sequence (3–5). However, this does not rule out the possibility that, depending on its conformation, Vβ CDR3 may in certain cases modulate SAG reactivity. For example, when the Vβ domain of TCR A6 (33) is superposed onto the 14.3.d Vβ domain in the VβCβ-SEB structure, SEB Tyr94 is predicted to contact Leu98 of A6 Vβ CDR3, located at the tip of this long protruding loop (not shown). Similar interactions may explain the observed influence of Vβ CDR3 residues on T cell reactivity toward MAM (149) and mouse retroviral Mtv-9 SAG (150). Alternatively, these SAGs may bind the TCR in different orientations than SEB. The latter possibility is supported by the finding that reactivity to the mouse retroviral SAG Mls-1 is affected by mutations at Vβ positions 19, 20, and 24, which are not part of the interface with SEB or SEC (3, 4, 151).

Conformational Changes in the TCR β–SEB Interface

The availability of high-resolution crystal structures for uncomplexed 14.3.d β chain (27) and SEB (9) permits an assessment of whether any conformational changes occur in Vβ or the SAG upon complex formation. The free and complexed Vβ domains superpose with a root-mean-square (RMS) difference of 0.33 Å for all α-carbon atoms. Likewise, the unbound and bound SEB molecules superpose with a RMS difference of 0.54 Å. Thus, there are no major rearrangements in the polypeptide backbones of Vβ or SEB associated with

complex formation, as also noted for the β-SEC3 complex (36). However, a number of adjustments in Vβ and SAG side-chain positions are evident when comparing the free and bound structures of the 14.3.d β chain and SEB. Certain of these changes are necessary to avoid steric clashes between the TCR and SAG, whereas others probably serve to maximize productive interactions between the two proteins. For example, the side chain of SEB residue Tyr91 undergoes a 120° rotation away from Vβ in order to avoid a collision with CDR2 (37). The structural rearrangements in the β-SEB interface are of similar magnitude to those observed in antigen-antibody complexes in which the antigen is a protein (146, 147, 152, 153). They imply a limited "induced fit" mechanism for TCR-SAG recognition analogous to that described for antigen-antibody interactions (152, 154). A further indication of flexibility in TCR-SAG association comes from the finding that the two β-SEB molecules in the asymmetric unit of the crystal, although similar, are not identical. A rotation of 6° is required to optimize the overlap between SEB molecules in the two complexes following superposition of their Vβ domains (37).

The changes in the conformation of interface residues in the 14.3.d β-SEB complex are not as large as those in the 2C TCR-dEV8/H-2K^b complex, in which the CDR1 and CDR3 loops of the Vα domain are displaced 4–6 Å relative to their positions in the unliganded 2C TCR structure (34). This probably indicates that the SAG has evolved to optimize its fit to the TCR. Indeed, calculations of shape complementarity (155) reveal that the β-SEB interface is about as tightly packed as antigen-antibody interfaces but significantly more tightly packed than TCR–peptide/MHC class I interfaces (33, 34, 156). It is important to emphasize, however, that, for both 2C TCR-dEV8/H-2K^b and 14.3.d TCR β–SEB complexes, the observed conformational changes are localized to the interfaces between the proteins and are not transmitted to the constant regions of the TCR. Thus, the possibility that changes in TCR conformation upon ligand binding are responsible for initiating T cell signaling can probably be ruled out. Rather, mechanisms based on ligand-induced TCR oligomerization (157) are more likely to account for T cell activation by peptide/MHC or SAGs.

Structural Basis for the Vβ-binding Specificity of SEB and SEC

The structure of the 14.3.d β chain–SEB complex explains why SEB recognizes certain Vβ families but not others. As discussed above, all the hydrogen bonds between SEB and mouse Vβ8.2 are formed between SEB side chains and Vβ main-chain atoms (Figure 2*B*, Table 1), such that the positions of these main-chain atoms should be similar in Vβ domains reactive with SEB but significantly different in Vβs that do not bind this SAG. A comparison of Vβ domains

of known three-dimensional structure confirms this expectation. Thus, SEB activates T cells bearing mouse Vβ8 and human Vβ12, but not mouse Vβ2 or Vβ5 (3). When human Vβ12.3 (33) is superposed onto mouse Vβ8.2 (Figure 4*A*, see color plates), the RMS difference in α-carbon positions for 14 residues in the SEB-binding site is only 0.9 Å. However, when mouse Vβ2.3 (30) is superposed onto mouse Vβ8.2 (Figure 4*B*), the RMS difference is 3.0 Å. This difference is largely attributable to a strand switch in Vβ2.3 relative to other Vβ domains of known structure: In Vβ2.3, the c$''$ strand is hydrogen bonded to the d strand of the adjacent (outer) β sheet, whereas in other Vβs the c$''$ strand is associated with the c$'$ strand in the same (inner) sheet (27, 29, 31, 33). A consequence of the c$''$ strand switch is a repositioning of CDR2 and FR3, which contribute 50% and 34%, respectively, of the total contacts to SEB. It is interesting that no bacterial or viral SAGs have been described with reactivity toward members of the mouse Vβ2 family (3), consistent with the unique folding topology of Vβ2.3. Similarly, when mouse Vβ5.2 (31) is superposed onto mouse Vβ8.2 (Figure 4*C*), the RMS difference in α-carbon positions for residues in the SEB-binding site is 2.1 Å. This difference is mainly attributable to a displacement of the c$''$ strand in a direction opposite from that of the c$''$ strand in the mouse Vβ2.3 domain, which again results in a repositioning of CDR2 and FR3. Except for MAM, which reacts with mouse Vβ5.1, no SAGs specific for members of the mouse Vβ5 family have been reported (3). These results indicate that the relative position of the c$''$ strand in Vβ domains is critical in determining their reactivity toward different microbial SAGs and suggest that Vβs reactive with SEB or SEC (mouse Vβ3, 7, 10, and 17; human Vβ3, 5, 12, 13, 14, 15, 17, and 20) probably have a β-strand topology in their SAG-binding sites similar to that of mouse Vβ8.2.

The structures of the β-SEB and β-SEC complexes also explain why T cells expressing mouse Vβ8.2 are stimulated by SEB, SEC1–3, and SPEA, but not by SEA, SED, SEE, TSST-1, or SPEC (3, 158). When SEC3 (12) is superposed onto SEB (9), the RMS difference in α-carbon positions for 11 residues in the TCR-binding site is only 0.51 Å (Figure 5*A*, see color plates). Although the three-dimensional structure of SPEA is not known, a sequence alignment with SEB and SEC reveals that it retains several key Vβ-contacting residues, in particular Asn60, Tyr90, and Gln210 (Figure 3*A*). Alanine-scanning mutagenesis has shown that these three residues are hot spots for the binding of SEC3 to the 14.3.d β chain (111), in agreement with the fact that SAGs having other residues at these positions display different Vβ-binding specificities. Thus, SEA, SED, SEE, SPEC, and TSST-1, which do not activate Vβ8.2-bearing T cells, differ from SEB at nearly all Vβ-contacting positions, in particular 90 and 210 (Figure 3*A*). Furthermore, when SEA (14) is superposed onto SEB, the RMS difference in β-carbon positions for residues in the TCR-binding site

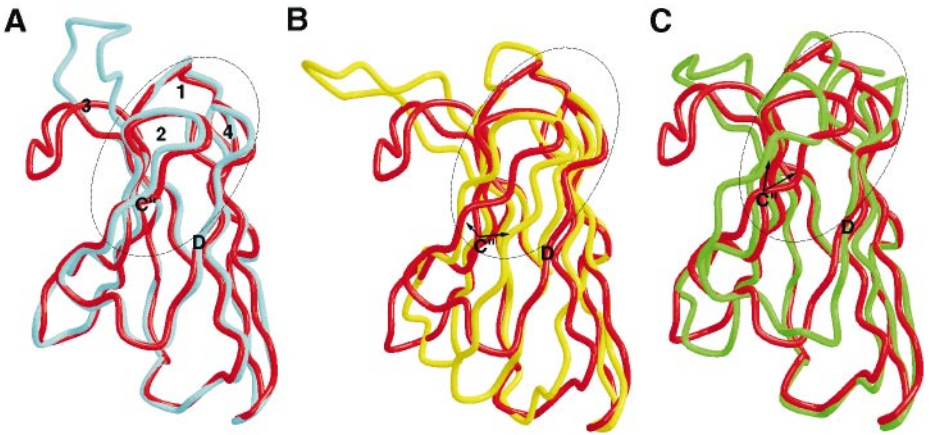

Figure 4 Comparison of Vβ structures in the region of the SAG-binding site. (*A*) Mouse Vβ8.2 (*red*) (27) superposed onto human Vβ12.3 (*blue*) (33). The CDR loops are numbered 1, 2 and 3; HV4 is labeled 4. (*B*) Mouse Vβ8.2 (*red*) superposed onto mouse Vβ2.3 (*yellow*) (30). (*C*) Mouse Vβ8.2 (*red*) superposed onto mouse Vβ5.2 (*green*) (31). The SEB-binding site of mouse Vβ8.2 is circled in each panel. The c$''$ and d strands are labeled.

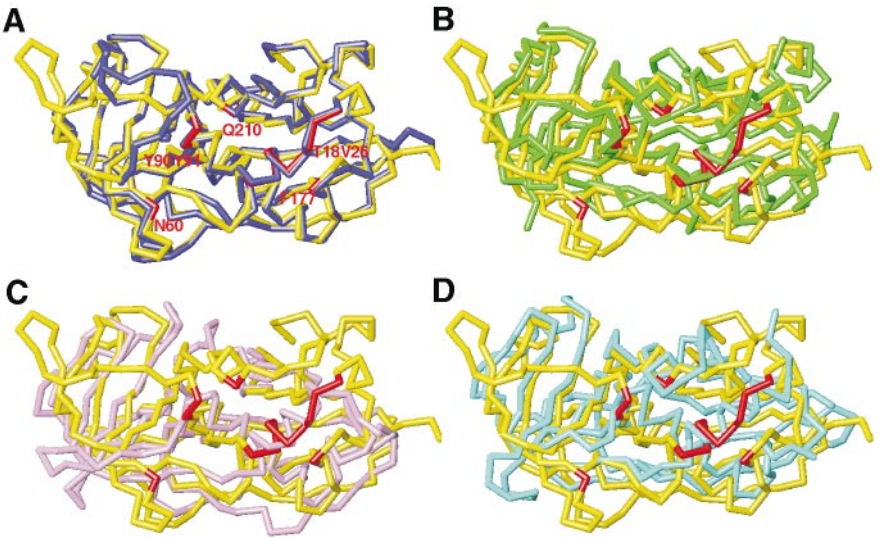

Figure 5 Structural comparison of SEB with other bacterial SAGs. SEB is oriented with its TCR-binding site directly facing the reader. (*A*) α-carbon diagram of SEB (*yellow*) (9) superposed onto SEC3 (*dark blue*) (12). (*B*) SEB (*yellow*) superposed onto SEA (*green*) (14). (*C*) SEB (*yellow*) superposed onto TSST-1 (*pink*) (1911). (*D*) SEB (*yellow*) superposed onto SPEC (*light blue*) (16). Regions of SEB in contact with Vβ in the 14.3.d β-SEB complex are *red*; key contact residues are labeled.

is 2.8 Å (Figure 5*B*). As shown in Figures 5*C* and *D*, the putative TCR-binding sites of TSST-1 (10, 11) and SPEC (16) are markedly different from that of SEB; this can account for the finding that the Vβ specificities of TSST-1 and SPEC do not overlap with those of SEB or SEC (3).

COMPARISON OF TCR-SAG-PEPTIDE/MHC AND TCR-PEPTIDE/MHC COMPLEXES

Although the three-dimensional structure of a TCR-SAG-peptide/MHC complex has not been determined, a model of this complex may be readily constructed by least-squares superposition of (*a*) the 14.3.d VβCβ-SEB complex, (*b*) the SEB–peptide/HLA-DR1 complex (122), and (*c*) the 2C TCR $\alpha\beta$ heterodimer (29), which uses the same Vβ element (mouse Vβ8.2) as does 14.3.d TCR (Figure 6*A*, see color). The accuracy of this model, in which the SAG is seen to bridge the APC and the T cell, depends on the assumption that there are no major conformational changes in any of the individual components upon complex formation; such changes are unlikely, given that none are observed in the TCR β-SEB or SEB-peptide/DR1 complexes (37, 122). This model may be compared with the structure of the 2C TCR complexed with peptide/MHC class I (34) (Figures 6*B* and *C*). Assuming that TCRs bind MHC class I and class II molecules in similar orientations, as recently argued on the basis of structural considerations (33), it is apparent that the binding of peptide/MHC to TCR in the TCR-peptide/MHC complex is different from that in the TCR-SEB-peptide/MHC complex and that there is only partial overlap between the binding sites on the TCR for SEB and for peptide/MHC. In the TCR-peptide/MHC complex (Figure 6*B*), the peptide antigen, as well as both the α1 and α2 helices of the class I molecule, simultaneously engage the TCR combining site. By contrast, in the model of the TCR-SEB-peptide/MHC complex (Figure 6*A*), the peptide is effectively removed from the TCR combining site, and there are no direct contacts between the TCR β chain and the MHC class II α1 or β1 (which corresponds to α2 in class I) helices. However, as discussed below, the MHC β1 helix is predicted to interact with the TCR Vα domain. In addition, the rotational orientation of TCR and MHC molecules in the TCR-SEB-peptide/MHC complex is different from that in the TCR-peptide/MHC complex (compare Figures 6*A* and *C*, respectively, in which the TCRs are shown in the same orientation): The MHC class II molecule in Figure 6*A* must be rotated approximately 40° counterclockwise around a vertical axis to align it with the MHC class I molecule in Figure 6*C*. Therefore, even though the TCR engages peptide/MHC differently in the two types of complexes, the end result—highly efficient T cell activation—is similar. This implies that the specific geometry of TCR engagement by peptide/MHC

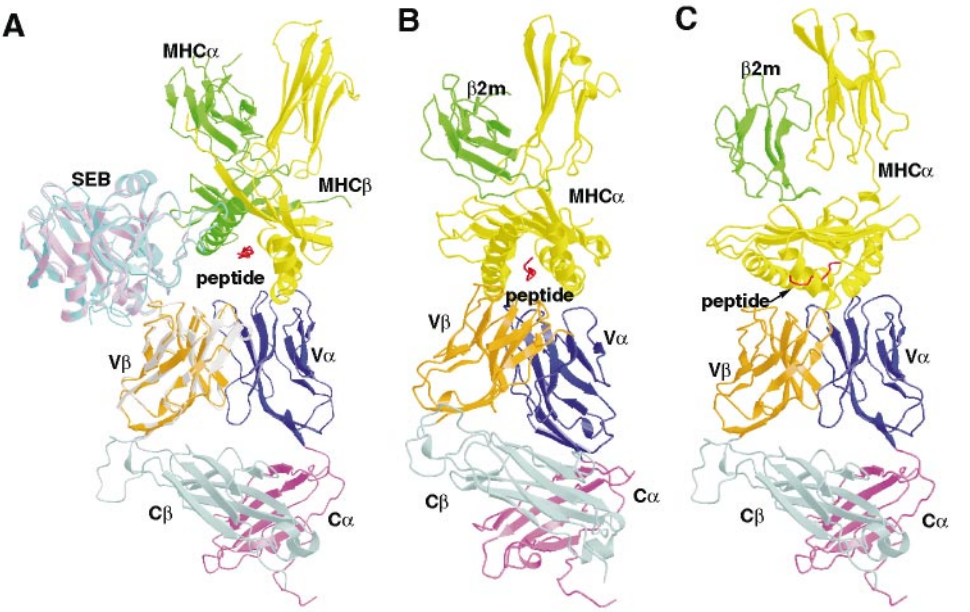

Figure 6 Comparison of TCR-SAG-peptide/MHC and TCR-peptide/MHC complexes. (*A*) Model of the TCR-SEB-peptide/MHC class II complex constructed by least-squares superposition of: 1) the 14.3.d VβCβ-SEB complex (37), 2) the SEB-peptide/HLA-DR1 complex (122), and 3) the 2C TCR $\alpha\beta$ heterodimer (29). (*B*) Structure of the 2C TCR-peptide/MHC class I complex (34). The complex is oriented such that the MHC molecule is approximately aligned with that in *panel A*. (*C*) Another view of the 2C TCR-peptide/MHC class I complex. The complex is oriented such that the TCRs in *panels A* and *C* are aligned.

may be less critical than are other factors, such as the affinity and kinetics of the binding reaction, in triggering T cells.

By acting as a wedge between the TCR β chain and the MHC class II α chain, the SAG is able to circumvent the normal mechanism for T cell triggering by specific peptide/MHC complexes. The result is polyclonal activation of whole populations of T cells expressing particular Vβ elements, largely irrespective of the peptide/MHC specificity of the corresponding TCRs. The absence of direct contacts between peptide and TCR in the model of the TCR-SEB–peptide/MHC class II complex in Figure 6*A* can explain the finding that formation of a TCR-SEB-DR1 complex was not affected by the presence of several different DR1-bound peptides (109). However, depending on the particular peptide bound by the MHC class II molecule, and on the conformations of the Vα and Vβ CDR3 loops, the peptide may in certain cases make a small number of contacts with the TCR and so modulate SAG activity.

It must be emphasized that other SAGs may bind differently to TCR and/or MHC class II than does SEB or SEC, thereby affecting the geometry of the TCR-SAG-peptide/MHC complex. In the case of TSST-1 bound to HLA-DR1 (Figure 1*B*), the SAG reaches across the antigen-binding groove, such that peptide-SAG and SAG-MHC β chain interactions may also contribute to complex stabilization (124). Furthermore, in contrast to SEB and SEC, the mode of binding of TSST-1 to DR1 would probably also preclude direct TCR-MHC interactions. This may represent an extreme example of the model in Figure 6*A* and illustrates how variations in the structure and positioning of the SAG wedge provide a means for different SAGs to modulate the degree of TCR-MHC interactions in the TCR-SAG-peptide/MHC complex.

Role of the TCR α Chain in Stabilization of the TCR-SAG-Peptide/MHC Complex

There is increasing evidence that the TCR α chain may, in certain cases, play a role in stabilizing the TCR-SAG-peptide/MHC complex and thereby influence T cell reactivity to bacterial or viral SAGs (5, 142, 159). For example, it was shown that Vα4 is expressed by Vβ6$^+$ T cell hybridomas that react with SEB but not by Vβ6$^+$ hybridomas that do not respond to this SAG (160). Transfection experiments demonstrated that the Vα4 α chain transferred SEB responsiveness regardless of whether the Vβ6 β chain was derived from a responsive or nonresponsive hybridoma (161). These effects of the TCR α chain on T cell activation by SAGs may be mediated through an interaction between Vα and the MHC class II β chain (5, 142, 161, 162). Thus, mutations at position 77 of the I-E^k β chain (141) and at positions 77 and 81 of HLA-DR1 β chain (140) were found to greatly reduce the T cell response to SEB without affecting binding of the SAG to MHC class II, which suggests contacts to the TCR. In addition,

the affinity of SEB for a soluble human TCR was observed to be significantly enhanced by the addition of soluble HLA-DR1 (109). These results may be understood in terms of the model of the TCR-SEB-peptide/MHC complex in Figure 6*A*, in which the Vα domain of the 2C TCR is predicted to interact with the MHC β1 helix. A close-up of putative contacts (<4 Å) between Vα CDR2 residues Ser51, Gly52, and Asp53 and the class II β chain residues Asp76 and Thr77 is shown in Figure 7*A* (see color plates). Thus, the overall stability of the TCR-SAG-peptide/MHC complex is probably determined by the combined strengths of three separate sets of interactions: TCR β chain–SAG, SAG–MHC α chain, and MHC β chain–TCR α chain.

The preferential expression of certain Vα regions among SAG-reactive T cells has been interpreted as evidence that these particular Vαs interact with MHC more favorably than do other Vαs during SAG-mediated T cell activation (5, 142, 159–161). The availability of crystal structures for several $\alpha\beta$ TCR heterodimers (29–31, 33) allows an examination of the possible effects of different TCR α chains on Vα-MHC interactions in the TCR-SAG-peptide/MHC complex. By superposing the Vβ domain of the 14.3.d β-SEB complex onto the Vβ domain of TCR A6 (33), N15 (31), or KB5-C20 (30), as described above for the 2C TCR, it is apparent that the extent of interaction between the Vα and MHC β1 domains in the TCR-SEB-peptide/MHC complex depends mostly on the relative orientation of Vα and Vβ domains in each TCR heterodimer. Because the variability in the geometry of Vα/Vβ association among these TCRs is considerable (2, 31), large differences are observed in the extent of Vα-MHC β1 interactions. These are illustrated in Figure 7. For the 2C TCR, as discussed above, Vα CDR2 Ser51, Gly52, and Asp53 are predicted to contact MHC β1 Asp76 and Thr77 (Figure 7*A*). For the A6 TCR, Vα CDR1 Gln30, and CDR2 Tyr50, Ser51 and Asn52 contact MHC β1 Glu69, Ala73, Asp76, Thr77, and His81 (Figure 7*B*). For the N15 TCR, Vα CDR1 Leu29 and CDR2 Thr51 contact MHC β1 Ala73, Thr77, and His81 (Figure 7*C*). For TCR KB-C50, no contacts are predicted because of the particular geometry of Vα/Vβ association of this TCR (not shown). In all cases where contacts between Vα and the MHC molecule are expected to occur, however, these involve Vα CDR2 and residues on the MHC β1 helix pointing away from the peptide-binding groove. Thus, depending on the geometry of Vα/Vβ association and on the structure of the Vα CDR2 loop, Vα-MHC class II interactions may (*a*) contribute to stabilizing the TCR-SEB-peptide/MHC complex and thus increase reactivity toward the SAG, (*b*) have no net effect on complex stability and not affect reactivity, or (*c*) destabilize the complex through unfavorable contacts and thereby decrease reactivity. In this way, the TCR α chain may modulate the level of activation by SEB of T cells expressing the same Vβ but different Vαs.

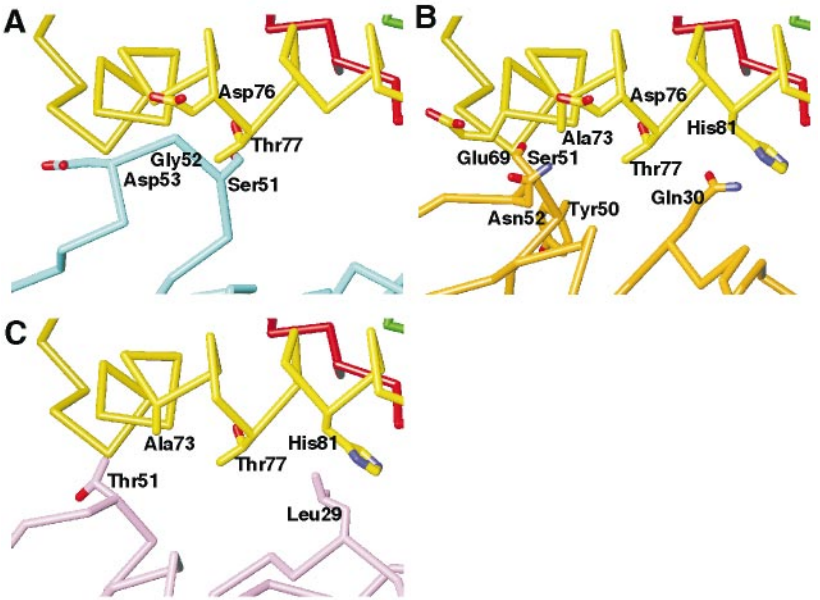

Figure 7 Differences in Vα-MHC β chain contacts as a result of differences in Vα/Vβ orientation and Vα CDR sequences. (*A*) Close-up of putative contacts between the MHC class II β chain (*yellow*) and Vα of the 2C TCR (*blue*) in the model of the TCR-SEB-peptide/MHC complex in Figure 6A. The bound peptide is *red*. Only those MHC and Vα residues predicted to form direct contacts are labeled. In the upper right hand corner is a portion of the MHC class II α chain in *green*. (*B*) Contacts between the MHC class II β chain and Vα of the A6 TCR (*orange*). The model of the TCR-SEB-peptide/MHC complex was constructed in the same way as that in Figure 7A, except using TCR A6 (33) instead of TCR 2C (29). The Vβ domain of TCR A6 was superposed onto 14.3.d Vβ by overlapping structurally equivalent FR residues. (*C*) Contacts between the MHC class II β chain and Vα of the N15 TCR (*pink*). The Vβ domain of TCR N15 (31) was superposed onto 14.3.d Vβ by overlapping structurally equivalent FR residues.

POTENTIAL THERAPEUTIC APPLICATIONS OF SUPERANTIGENS

Because bacterial SAGs are such extremely potent activators of the immune system, efforts are currently underway in a number of laboratories to engineer them for therapeutic applications (163). Knowledge of the three-dimesional structure of SAGs, and of their binding sites for TCR and MHC, may be used to design variants with altered binding properties toward these ligands, resulting in desired biological effects. The potential applications of SAG derivatives include cancer immunotherapy and the treatment of infectious and autoimmune diseases.

The recruitment of antigen-specific cytotoxic T lymphocytes (CTLs) is a major goal for the immunotherapy of malignant tumors. However, the frequency of tumor-specific CTLs is generally too low to interfere with progressive tumor growth. An attractive approach for immunotherapy is to use antibodies specific for tumor-associated antigens to target large numbers of T cells to the tumor. Taking advantage of the ability of SAGs to activate large populations of T cells, chemical conjugates of SEA and the colon carcinoma–reacting monoclonal antibodies (mAbs) C215 or C242 were shown to mediate T cell–dependent destruction of colon carcinoma cells lacking MHC class II molecules (164). The SEA-mAb–mediated cytotoxicity was MHC class II independent and did not require antigen-specific effector CTLs. In subsequent work, a recombinant fusion protein of SEA and the Fab region of the C215 mAb was found to efficiently target T cells to lyse $C215^+$ MHC class II–negative human colon carcinoma cells (165). Treatment of mice carrying B16 melanoma cells expressing transfected C215 antigen resulted in 85–99% inhibition of tumor growth and allowed long-term survival. In similar experiments, SEA bound to specific anti-carcinoma cell or anti-ganglioside GD2 mAbs displayed T cell–mediated cytotoxicity toward MHC class II–negative lymphatic leukemia cell lines or neuroblastoma cells, respectively (166, 167). The demonstration of a Zn^{2+}-dependent MHC class II binding site with high affinity in the large domain of SEA (14, 128, 129), which is distinct from the low-affinity SEB-like binding site in the small domain, prompted the introduction of a point mutation (Asp227 → Ala) in the high-affinity site in order to lower the systemic toxicity of Fab-SEA conjugates (168). Thus, after treatment with Fab-SEA Asp227 → Ala, a 100- to 1000-fold reduction in serum levels of IL-6 and TNF was observed in mice compared with the wild-type conjugate, without affecting anti-tumor activity. These results suggest that bacterial SAGs can be converted into tolerable immunotoxins for cancer therapy (169).

Inactivated forms of SAGs might be useful as vaccines to protect against staphylococcal or streptococcal toxic shock. Mutants of SEB that do not bind TCR do not induce T cell proliferation and therefore do not cause toxic shock (170). Animals immunized with mutants of SEA with attenuated binding to TCR or MHC class II developed high titers of anti-SEA antibodies and were fully protected against challenge with the wild-type toxin (171). Formalinized SEB toxoid–containing microspheres have been tested for efficacy in rhesus monkeys as a vaccine candidate for respiratory toxicosis and toxic shock (172). Protective immunity correlated with antibody levels in both the circulation and the respiratory tract. Similar results were obtained with intranasal or intramuscular immunization by using meningococcal outer-membrane protein proteasome-SEB toxoid. The proteosome-SEB toxoid vaccine was efficacious in protecting 100% of monkeys against severe symptomatology and death from aerosolized-SEB intoxication (173).

T cell activation by SAGs is generally followed by the disappearance or inactivation of the responding T cells, resulting in clonal deletion of cells bearing specific Vβ elements (3, 4). Chronic exposure to low concentrations of SAGs permits clonal deletion to occur directly, without the cells first passing through a state of hyperreactivity (174, 175). In mice with EAE or lupus nephritis, both of which serve as models for human autoimmune diseases, treatment with SEB resulted in a reduction in symptoms or in a cure of the disease (176–179). In both models, autoimmunity is known to be mediated by self-reactive T cells expressing a single Vβ element (mouse Vβ8), such that the effect of the SAG most likely results from the specific elimination of pathogenic T cells bearing that particular Vβ. These experiments suggest that SAGs could potentially be used for the prevention of autoimmune disease by selectively eliminating specific T cell populations. In cases where T cells from several Vβ families might be involved in the disease process, SAGs engineered to recognize these Vβs could be used for therapy. Knowledge of the three-dimensional structure of TCR-SAG complexes should facilitate the design of SAGs with predefined Vβ specificities.

A number of concerns must be addressed, however, before SAGs can be used as therapeutic agents (180). Administration of SAGs may lead to the release of dangerous levels of cytokines such as TNF, resulting in toxic shock. In addition, inadvertent stimulation of autoreactive T cells could trigger autoimmune disease. It appears likely, however, that the systemic toxicity of SAGs can be dissociated from the superantigenic effects of these molecules through structure-based genetic engineering, as described above for SEA-Fab conjugates (168) and SEA vaccines (171). Similarly, mutations of TSST-1 have been described that alter either lethality or superantigenicity, without significantly affecting the other property (181–183).

FUTURE DIRECTIONS

Although the X-ray crystallographic studies described above represent important advances in our understanding of SAG interactions with TCR and MHC, the apparent diversity of these interactions clearly illustrates the need for further work in this area. For example, TSST-1 binds differently to MHC class II molecules than does SEB (Figure 1) (122–124), and its interaction with the TCR presumably differs as well. Unlike SEB and TSST-1, which have only one class II–binding site, mutagenesis and biochemical experiments indicate that SEA has two such sites (127–129). However, because the crystal structure of an SEA–MHC class II complex has not been determined, the precise locations of these sites are unknown. SED and SPEC crystallize as homodimers (15–16), which may facilitate TCR oligomerization and T cell triggering. However, X-ray crystallographic studies are required to elucidate the geometry of the putative SED_2TCR_2, SED_2MHC_2, $SPEC_2TCR_2$, and $SPEC_2MHC_2$ tetramers. Our knowledge of SAG structure is currently limited to the staphylococcal and streptococcal pyrogenic toxins (9–16) and to a staphylococcal exfoliative toxin (17, 18). No structural information is available for SAGs produced by mycoplasma, such as MAM (19), or by viruses (22–26), including the much-studied MMTV SAGs. Human endogenous retroviral SAGs that are associated with autoimmune diseases (26) may become a focus of future attention. Finally, the structures of entire TCR-SAG-MHC complexes must be determined in order to define experimentally the putative Vα-MHC interactions discussed in this review.

X-ray crystallographic studies of TCR-SAG, SAG-MHC, and TCR-SAG-MHC complexes will open the way for the design of SAG variants with altered binding properties for TCR and MHC for use as tools in dissecting structure-activity relationships in this system. The relative contributions of TCR-SAG and SAG-MHC interactions to T cell stimulation can be defined by engineering panels of mutant SAGs with both higher and lower affinities for TCR and MHC than the wild-type toxins have. It has been shown that SAGs mimic the interaction of peptide/MHC complexes with the TCR in terms of affinities and kinetics (109–112). It remains to be established, however, whether there is an optimum affinity for T cell activation by SAGs (or by peptide/MHC), as predicted by the serial triggering (118, 119) and kinetic proofreading (120) models of T cell activation, such that SAGs with either higher or lower affinities than this optimum value exhibit decreased ability to stimulate T cells. Alternatively, SAGs with progressively higher affinities for the TCR relative to the wild type may stimulate T cells increasingly well, until some plateau of maximum stimulation is attained. Mutants with altered affinities for the TCR can be used to distinguish between these possibilities and thereby define the affinity and kinetic

parameters governing T cell activation by SAGs. The role, if any, of cooperative interactions involving the TCR α chain in stabilizing the TCR-SAG-MHC complex can be similarly addressed. By thus combining X-ray crystallography with mutagenesis and binding studies, a comprehensive understanding of the physical basis of T cell activation by microbial SAGs should emerge.

ACKNOWLEDGMENTS

This research was supported by NIH grants AI36900 and AI42937 and National Multiple Sclerosis Society grant RG2747 to RAM. ELM is supported by grants from CONICET, UBA, and Fundacin Antorchas. We thank IA Wilson for coordinates of the 2C TCR-dEV8/H-2K^b complex, CV Stauffacher for coordinates of SEC3, EN Baker and J Fraser for coordinates of SPEC, and DC Wiley for coordinates of the TSST-1/HLA-DR1 complex.

Literature Cited

1. Bentley GA, Mariuzza RA. 1995. The structure of the T cell antigen receptor. *Annu. Rev. Immunol.* 14:563–90
2. Wilson IA, Garcia KC. 1997. T-cell receptor structure and TCR complexes. *Curr. Opin. Struct. Biol.* 7:839–48
3. Kotzin BL, Leung DYM, Kappler J, Marrack P. 1993. Superantigens and their potential role in human disease. *Adv. Immunol.* 54:99–166
4. Scherer MT, Ignatowicz L, Winslow GM, Kappler JW, Marrack P. 1993. Superantigens: bacterial and viral proteins that manipulate the immune system. *Annu. Rev. Cell. Biol.* 9:101–128
5. Webb SR, Gascoigne NRJ. 1994. T-cell activation by superantigens. *Curr. Opin. Immunol.* 6:467–475
6. Bohach GA, Fast DJ, Nelson RD, Schlievert PM. 1990. Staphylococcal and streptococcal pyrogenic toxins involved in toxic shock syndrome and related illnesses. *Crit. Rev. Microbiol.* 17:251–272
7. Betley MJ, Borst DW, Regassa LB. 1992. Staphylococcal enterotoxins, toxic shock syndrome toxin and streptococcal pyrogenic exotoxins: a comparative study of their molecular biology. *Chem. Immunol.* 55:1–35
8. Bohach GA. 1997. Staphylococcal enterotoxins B and C. In *Superantigens: Molecular Biology, Immunology and Relevance to Human Disease*, ed. DYM Leung, BT Huber, PM Schlievert, Marcel Dekker Inc. NY, pp. 167–198
9. Swaminathan S, Furey W, Pletcher J, Sax M. 1992. Crystal structure of staphylococcal enterotoxin B, a superantigen. *Nature* 359:801–806
10. Prasad GS, Earhart CA, Murray DL, Novick RP, Schlievert PM, Ohlendorf DH. 1993. Structure of toxic shock syndrome toxin–1. *Biochemistry* 32:13761–13766.
11. Acharya KR, Passalacqua EF, Jones EY, Harlos K, Stuart DI, Brehm RD, Tranter HS. 1994. Structural basis of superantigen action inferred from crystal structure of toxic–shock syndrome toxin–1. *Nature* 367:94–97
12. Hoffmann ML, Jablonski LM, Crum KK, Hackett SP, Chi Y–I, Stauffacher CV, Stevens DL, Bohach GA. 1994. Predictions of T cell receptor and major histocompatibility complex binding sites on staphylococcal enterotoxin C3. *Infect. Immun.* 62:3396–3407
13. Papageorgiou A, Acharya KR, Shapiro R, Passalacqua EF, Brehm RD, Tranter HS. 1995. Crystal structure of the superantigen enterotoxin C2 from *Stapylococcus aureus* reveals a zinc–binding site. *Structure* 3:769–779
14. Schad EM, Zaitseva I, Zaitsev VN, Dohlsten M, Kalland T, Schlievert PM, Ohlendorf DH, Svensson LA. 1995.

Crystal structure of the superantigen staphylococcal enterotoxin type A. *EMBO J.* 14:3292–3301

15. Sundstrom M, Abrahmsen L, Antonsson P, Mehindate K, Mourad W, Dohlsten M. 1996. The crystal structure of staphylococcal enterotoxin type D reveals Zn^{2+}–mediated homodimerization. *EMBO J.* 15:6832–6840
16. Roussell A, Anderson BF, Baker HM, Fraser JD, Baker EN. 1997. Crystal structure of the streptococcal superantigen SPE–C: dimerization and zinc–binding suggest a novel mode of interaction with MHC class II molecules. *Nature Struct. Biol.* 4:635–643
17. Vath GM, Earhart CA, Rago JV, Kim MH, Bohach GA, Schlievert PM, Ohlendorf DH. 1997. The structure of the superantigen exfoliative toxin A suggests a novel regulation as a serine protease. *Biochemistry* 36:1559–1566
18. Cavarelli J, Prevost G, Bourguet W, Moulinier L, Chevrier B, Delagoutte B, Bilwes A, Mourey L, Rifau S, Piemont Y, Moras D. 1997. The structure of *Staphylococcus aureus* epidermolytic toxin A, an atypic serine protease, at 1.7 Å resolution. *Structure* 5:813–824
19. Cole BC, Griffiths MM. 1993. Triggering and exacerbation of autoimmune arthritis by the *Mycoplasma arthritidis* superantigen MAM. *Arthritis Rheumat.* 36:994–1002
20. Ito Y, Abe J, Yoshino K, Takeda T, Koshaka T. 1995. Sequence analysis of the gene for a novel superantigen produced by *Yersinia pseudotuberculosis* and expression of the recombinant protein. *J. Immunol.* 154:5896–5906
21. Miyoshi–Akiyama T, Abe A, Kato H, Kawahara K, Narimatsu H, Uchiyama T. 1995. DNA sequencing of the gene encoding a bacterial superantigen, *Yersinia pseudotuberculosis*–derived mitogen (YPM), and characterization of the gene product, cloned YPM. *J. Immunol.* 154:5228–5234
22. Acha–Orbea H, MacDonald HR. 1995. Superantigens of mouse mammary tumor virus. *Annu. Rev. Immunol.* 13:459–486
23. Astoul E, Lafage M, Lafon M. 1996. Rabies superantigen as a Vβ T–dependent adjuvant. *J. Exp. Med.* 183:1623–1631
24. Dobrescu D, Ursea B, Pope M, Asch AS, Posnett DM. 1995. Enhanced HIV–1 replication in Vβ12 T cells due to human cytomegalovirus in monocytes: evidence for a putative herpesvirus superantigen. *Cell* 82:753–763
25. Sutkowski N, Palkama T, Ciurli C, Sekal R–P, Thorley–Lawson DA, Huber B. 1996. An Epstein–Barr virus–associated superantigen. *J. Exp. Med.* 184:971–980
26. Conrad B, Weissmahr RN, Boni J, Arcari R, Schupbach J, Mach B. 1997. A human endogenous retroviral superantigen as candidate autoimmune gene in type I diabetes. *Cell* 90:303–313
27. Bentley GA, Boulot G, Karjalainen K, Mariuzza RA. 1995. Crystal structure of the β chain of a T cell antigen receptor. *Science* 267:1984–1987
28. Fields BA, Ober B, Malchiodi EL, Lebedeva MI, Braden B, Ysern X, Kim J–K, Shao X, Ward ES, Mariuzza RA. 1995. Crystal structure of the Vα domain of a T cell antigen receptor. *Science* 270: 1821–1824
29. Garcia KC, Degano M, Stanfield RL, Brunmark A, Jackson MR, Peterson PA, Teyton L, Wilson IA. 1996. An $\alpha\beta$ T cell receptor structure at 2.5 Å and its orientation in the TCR–MHC complex. *Science* 274:209–219
30. Housset D, Mazza G, Gregoire C, Piras C, Malissen B, Fontecilla–Camps JC. 1997. The three–dimensional structure of a T-cell antigen receptor VαVβ heterodimer reveals a novel arrangement of the Vβ domain. *EMBO J.* 16:4205–4216
31. Wang J, Lim K, Smolyar A, Teng M, Liu J, Tse AGD, Liu J, Hussey RE, Chishti Y, Thomson CTT, Sweet RM, Nathenson SG, Chang H, Sacchettini JC, Reinherz EL. 1998. Atomic structure of an $\alpha\beta$ T cell receptor (TCR) heterodimer in complex with an anti–TCR Fab fragment derived from a mitogenic antibody. *EMBO J.* 17:10–26
32. Li H, Lebedeva MI, Llera AS, Fields BA, Brenner MA, Mariuzza RA. 1998. Structure of the Vδ domain of a human $\gamma\delta$ T-cell antigen receptor. *Nature* 391:502–506
33. Garboczi DN, Ghosh P, Utz U, Fan QR, Biddison WE, Wiley DC. 1996. Structure of the complex between human T-cell receptor, viral peptide and HLA–A2. *Nature* 384:134–141
34. Garcia KC, Degano M, Pease LR, Huang M, Peterson PA, Teyton L, Wilson IA. 1998. Structural basis of plasticity in T cell receptor recognition of a self peptide–MHC antigen. *Science* 279: 1166–1172
35. Ding Y–H, Smith KJ, Garboczi DN, Utz U, Biddison WE, Wiley DC. 1998. Two human T cell receptors bind in a similar diagonal mode to the HLA–A2/Tax

peptide complex using different TCR amino acids. *Immunity* 8:403–411
36. Fields BA, Malchiodi EL, Li H–M, Ysern X, Stauffacher CV, Schlievert PM, Karjalainen K, Mariuzza RA. 1996. Crystal structure of the β chain of a T-cell receptor complexed with a superantigen. *Nature* 384:188–192
37. Li H, Llera A, Tsuchiya D, Leder L, Ysern X, Schlievert PM, Karjalainen K, Mariuzza RA. 1998. Three–dimensional structure of the complex between a T cell receptor β chain and the superantigen staphylococcal enterotoxin B. *Immunity*
38. MacDonald HR, Lees RK, Baschieri S, Herrmann T, Lussow AR. 1993. Peripheral T-cell reactivity to bacterial superantigens *in vivo*: the response/anergy paradox. *Immunol. Rev.* 133:105–117
39. Woodland DL, Wen R, Blackman MA. 1997. Why do superantigens care about peptides? *Immunol. Today* 18:18–22
40. Kappler JW, Roehm N, Marrack P. 1987. T cell tolerance by clonal elimination in the thymus. *Cell* 49:273–280
41. MacDonald HR, Schneider R, Lees RK, Howe RC, Acha-Orbea H, Festenstein H, Zinkernagel RM, Hengartner H. 1988. T-cell receptor Vβ use predicts reactivity and tolerance to Mlsa–encoded antigens. *Nature* 332:40–45
42. Pullen AM, Bill J, Kubo RT, Marrack P, Kappler JW. 1991. Analysis of the interaction site for the self superantigen Mls–1a on T cell receptor Vβ. *J. Exp. Med.* 173:1183–1192
43. White J, Herman A, Pullen AM, Kubo R, Kappler JW, Marrack P. 1989. The Vβ–specific superantigen staphylococcal enterotoxin B: stimulation of mature T cells and clonal deletion in neonatal mice. *Cell* 56:27–35
44. Rellahan BL, Jones LA, Kruisbeek AM, Fry AM, Matis LA. 1990. *In vivo* induction of anergy in peripheral V$\beta 8^+$ T cells by staphylococcal enterotoxin B. *J. Exp. Med.* 172:1091–1100
45. O'Hehir RE, Lamb JR. 1990. Induction of specific clonal anergy in human T lymphocytes by *Staphylococcus aureus* enterotoxins. *Proc. Natl. Acad. Sci. USA* 87:8884–8888
46. Kawabe Y, Ochi A. 1991. Programmed cell death and extrathymic reduction of V$\beta 8^+$ CD4$^+$ T cells in mice tolerant to *Staphylococcus aureus* enterotoxin B. *Nature* 349:245–248
47. Golovkina TV, Chervonsky A, Dudley JP, Ross SR. 1992. Transgenic mouse mammary tumor virus superantigen expression prevents viral infection. *Cell* 69:637–645
48. Held W, Waanders G, Shakov AN, Scarpellino L, Acha–Orbea H, MacDonald HR. 1993. Superantigen–induced immune stimulation amplifies mouse mammary tumor virus infection and allows virus transmission. *Cell* 74:529–540
49. Ignatowicz L, Kappler J, Marrack P. 1992. The effects of chronic infection with a superantigen–producing virus. *J. Exp. Med.* 175:917–923
50. Golovkina TV, Dudley JP, Jaffe A, Ross SR. 1995. Mouse mammary tumor viruses with functional superantigen genes are selected during *in vivo* infection. *Proc. Natl. Acad. Sci. USA* 92:4828–4832
51. Wrona TJ, Lozano M, Binhazim AA, Dudley JP. 1998. Mutational and functional analysis of the C–terminal region of the C3H mouse mammary tumor virus superantigen. *J. Virol.* 72:4746–4755
52. Deresiewicz RL. 1997. Staphylococcal toxic shock syndrome. In *Superantigens: Molecular Biology, Immunology and Relevance to Human Disease*, ed. DYM Leung, BT Huber, PM Schlievert, Marcel Dekker Inc. NY, pp. 435–479
53. Stevens DL. 1997. Streptococcal toxic shock syndrome. In *Superantigens: Molecular Biology, Immunology and Relevance to Human Disease*, ed. DYM Leung, BT Huber, PM Schlievert, Marcel Dekker Inc. NY, pp. 481–501
54. Rago JV, Schlievert PM. 1998. Mechanisms of pathogenesis of staphylococcal and streptococcal superantigens. *Curr. Top. Microbiol. Immunol.* 225:81–97
55. Alber G, Hammer DK, Fleischer B. 1990. Relationship between enterotoxic– and T lymphocyte–stimulating activity of staphylococcal enterotoxin. *Br. J. Immunol.* 144:4501–4506
56. Harris TO, Grossman D, Kappler JW, Marrack P, Rich RR, Betley MJ. 1993. Lack of complete correlation between emetic and T cell stimulatory activities of staphylococcal enterotoxins. *Infect. Immun.* 61:3175–3183
57. Hovde CJ, Marr JC, Hoffmann ML, Hackett SP, Chi YI Crum KK, Stevens DL, Stauffacher CV, Bohach GA. 1994. Investigation of the role of the disulphide bond in the activity and structure of staphylococcal enterotoxin C1. *Mol. Microbiol.* 13:897–909
58. Sears CL, Kaper JB. 1996. Enteric bacterial toxins: mechanisms of action and linkage to intestinal secretion. *Microbiol. Rev.* 60:167–215
59. Hamad ARA, Marrack P, Kappler JW. 1997. Transcytosis of staphylococcal

superantigen toxins. *J. Exp. Med.* 185: 1447–1454
60. Rose NR, Wolfgram LJ, Herskowitz A, Beisel KW. 1986. Postinfectious autoimmunity: two distinct phases of coxsackie B3–induced myocarditis. *Ann. N.Y. Acad. Sci.* 475:146–156
61. Ray CG, Palmer JP, Crossley JR, Williams RH. 1980. Coxsackie B virus antibody responses in juvenile–onset diabetes mellitus. *Clin. Endocrinol.* 12:375–378
62. Oldstone MBA. 1990. Molecular mimicry and autoimmune disease. *Cell* 50: 819–820
63. Wucherpfenning KW, Strominger JL. 1995. Molecular mimicry in T-cell mediated autoimmunity: viral peptides activate human T cell clones specific for myelin basic protein. *Cell* 80:695–705
64. Hemmer B, Fleckenstein BT, Vergelli M, Jung G, McFarland H, Martin R. 1997. Identification of high potency microbial and self ligands for a human autoreactive class II–restricted T cell clone. *J. Exp. Med.* 185:1651–1659
65. Renno T, Acha–Orbea H. 1996. Superantigens in autoimmune disease: still more shades of gray. *Immunol. Rev.* 154: 175–191
66. Bach JF. 1995. T cell receptor use in organ–specific human autoimmune diseases other than rheumatoid arthritis and multiple sclerosis. *Ann. N.Y. Acad. Sci.* 756:453–459
67. Traugott U. 1987. Multiple sclerosis: relevance of class I and class II MHC–expressing cells to lesion development. *J. Neuroimmunol.* 16:283–302
68. Olerup O, Hillert J. 1990. HLA class II associated genetic susceptibility in multiple sclerosis: a critical evaluation. *Tissue Antigens* 38:1–5
69. Allegretta M, Nicklas JA, Sriram S, Albertini RJ. 1990. T cells responsive to myelin basic protein in patients with multiple sclerosis. *Science* 247:718–721
70. Wucherpfennig KW, Zhang J, Witek C, Matsui M, Modabber Y, Ota K, Hafler DA. 1994. Clonal expansion and persistence of human T cells specific for an immunodominant myelin basic protein peptide. *J. Immunol.* 150:5581–5592
71. Zhang J, Markovic S, Lacet B, Raus J, Weiner HL, Hafler DA. 1994. Increased frequency of interleukin 2–responsive T cells specific for myelin basic protein and proteolipid protein in peripheral blood and cerebrospinal fluid of patients with multiple sclerosis. *J. Exp. Med.* 179: 973–984
72. Stinissen P, Raus J, Zhang J. 1997. Autoimmune pathogenesis of multiple sclerosis: role of autoreactive T lymphocytes and new immunotherapeutic strategies. *Crit. Rev. Immunol.* 17:33–75
73. Brocke S, Gaur A, Piercy C, Gautam K, Gijbels C, Fathman CG, Steinman L. 1993. Induction of relapsing paralysis in experimental autoimmune encephalomyelitis by bacterial superantigen. *Nature* 365:642–644
74. Racke MK, Quigley L, Cannella B, Raine C, McFarlin DE, Scott DE. 1994. Superantigen modulation of experimental allergic encephalomyelitis: activation or anergy determines outcome. *J. Immunol.* 152:2051–2059
75. Brocke S, Hausmann S, Steinman L, Wucherpfennig KW. 1998. Microbial peptides and superantigens in the pathogenesis of autoimmune diseases of the central nervous system. *Sem. Immunol.* 10:57–67
76. Paliard X, West SG, Lafferty JA, Clements JR, Kappler JW, Marrack P, Kotzin BL. 1991. Evidence for the effects of a superantigen in rheumatoid arthritis. *Science* 253:325–329
77. Haqqi TM, Anderson GD, Banerjee S, David CS. 1992. Restricted heterogeneity in T-cell antigen receptor Vβ gene usage in the lymph nodes and arthritic joints of mice. *Proc. Natl. Acad. Sci. USA* 89:1253–1255
78. Osman GE, Toda M, Kanagawa O, Hood LE. 1993. Characterization of the T cell receptor repertoire causing collagen arthritis in mice. *J. Exp. Med.* 177:387–395
79. Chiocchia G, Boissier MC, Fournier C. 1991. Therapy against murine collagen–induced arthritis with T-cell receptor Vβ–specific antibodies. *Eur. J. Immunol.* 21:2899–2905
80. Moder KG, Luthra HS, Griffiths M, David CS. 1993. Prevention of collagen–induced arthritis in mice by depletion of T cell receptor Vβ8 bearing T cells with monoclonal antibodies. *Br. J. Rheumat.* 32:26–30
81. Kumar V, Sercarz E. 1993. The involvement of T cell receptor peptide–specific regulatory $CD4^+$ T cells in recovery from antigen–induced autoimmune disease. *J. Exp. Med.* 178:909–916
82. Kumar V, Stellrecht K, Sercarz E. 1996. Inactivation of CD4 regulatory T cells results in chronic autoimmunity. *J. Exp. Med.* 184:1609–1617
83. Kumar V, Aziz F, Sercarz E, Miller A. 1997. Regulatory T cells specific for the

same framework 3 region of the Vβ8.2 chain are involved in the control of collagen II–induced arthritis and experimental autoimmune encephalomyelitis. *J. Exp. Med.* 185:1725–1733

84. Singh B, Prange S, Jevnikar AM. 1998. Protective and destructive effects of microbial infection in insulin–dependent diabetes mellitus. *Sem. Immunol.* 10:79–86
85. Conrad B, Weldmann E, Trucco G, Rudert WA, Behboo R, Ricordi C, Rodriquez-Rilo H, Finegold D, Trucco M. 1994. Evidence for superantigen involvement in insulin–dependent diabetes mellitus aetiology. *Nature* 371:351–355
86. Luppi P, Trucco M. 1996. Superantigens in insulin–dependent diabetes mellitus. *Springer Semin. Immunopathol.* 17:333–362
87. Abe J, Kotzin BL, Jujo K, Melish ME, Glode MP, Kohsaka T, Leung DY. 1992. Selective expansion of T cells expressing T-cell receptor variable region Vβ2 and Vβ8 in Kawasaki disease. *Proc. Natl. Acad. Sci. USA* 89:4066–4070
88. Abe J, Kotzin BL, Meissner C, Melish ME, Takahashi M, Fulton D, Romagne F, Malissen B, Leung DYM. 1993. Characterization of T cell receptor changes in acute Kawasaki disease. *J. Exp. Med.* 177:791–796
89. Curtis N, Zheng R, Lamb JR, Levin M. 1995. Evidence for a superantigen–mediated process in Kawasaki disease. *Arch. Dis. Child.* 72:308–311
90. Leung DY, Giorno RC, Kazemi LV, Flynn PA, Busse JB. 1995. Evidence for superantigen involvement in cardiovascular injury due to Kawasaki syndrome. *J. Immunol.* 155:5018–5021
91. Leung DY, Meissner HC, Fulton DR, Murray DL, Kotzin BL, Schlievert PM. 1993. Toxic shock syndrome toxin–secreting *Staphylococcus aureus* in Kawasaki syndrome. *Lancet* 342:1385–1388
92. Pietra BA, De Inocencio J, Giannini EH, Hirsch R. 1994. TCR V beta family repertoire and T cell activation markers in Kawasaki disease. *J. Immunol.* 153:1881–1888
93. Sakaguchi M, Kato H, Nishiyori A, Sagawa K, Itoh K. 1995. Characterization of $CD4^+$ T helper cells in patients with Kawasaki disease (KD): preferential production of tumor necrosis factor–alpha (TNF–alpha) by Vbeta2 or Vbeta8 $CD4^+$ T helper cells. *Clin. Exp. Immunol.* 99:276–282
94. Jason J, Montana E, Donald JF, Seidman M, Inge KL, Campbell R. 1998. Kawasaki disease and the T-cell antigen receptor. *Hum. Immunol.* 59:29–38
95. Iandolo JJ, Chapes SK. 1997. The exfoliative toxins of *Staphylococcus aureus*. In *Superantigens: Molecular Biology, Immunology and Relevance to Human Disease*, ed. DYM Leung, BT Huber, PM Schlievert, Marcel Dekker Inc. NY, pp. 231–255
96. Prevost G, Rifai S, Chaix ML, Piemont Y. 1991. Functional evidence that the Ser–195 residue of staphylococcal exfoliative toxin A is essential for biological activity. *Infect. Immun.* 59:3337–3339
97. Henderson CA, Highet AS. 1988. Acute psoriasis associated with Lancefield group C and group G cutaneous streptococcal infections. *Br. J. Dermatol.* 118: 559–562
98. Lewis HM, Baker BS, Bokth S, Powles AV, Garioch JJ, Valdimarsson H, Fry L. 1993. Restricted T cell receptor Vβ gene usage in the skin of patients with guttate and chronic plaque psoriasis. *Br. J. Dermatol.* 129:514–520
99. Chang JCC, Smith LR, Froning KJ, Schwabe BJ, Laxer JA, Caralli LL, Kurland HH, Karasek MA, Wilkinson DI, Carlo DJ, Brostoff SW. 1994. $CD8^+$ T cells in psoriatic lesions preferentially use T-cell receptor Vbeta 3 and/or Vbeta 13.1 genes. *Proc. Natl. Acad. Sci USA* 91:9282–9286
100. Leung DYM, Travers JB, Giorno R, Norris DA, Skinner R, Aelion J, Kazemi LV, Kim MH, Trumble AE, Kotb M, Schlievert PM. 1995. Evidence for streptococcal superantigen–driven process in acute guttate psoriasis. *J. Clin. Invest.* 96:2106–2112
101. Boehncke WH, Dressel D, Manfras B, Zollner TM, Wettstein A, Bohm BO, Sterry W. 1995. T-cell repertoire in chronic plaque–stage psoriasis is restricted and lacks enrichment of superantigen–associated Vβ regions. *J. Invest. Dermatol.* 104:725–728
102. Sayama K, Midorikawa K, Hanakawa Y, Sugai M, Hashimoto K. 1998. Superantigen production by *Staphylococcus aureus* in psoriasis. *Dermatology* 196:194–198
103. Leung DY. 1995. Atopic dermatitis: the skin as a window into the pathogenesis of chronic allergic diseases. *J. Allergy Clin. Immunol.* 96:302–318
104. Leyden JJ, Marples RR, Klingman AM. 1974. *Staphylococcus aureus* in the lesions of atopic dermatitis. *Br. J. Dermatol.* 90:525–530

105. Leung DY, Harbeck R, Bina P, Reiser RF, Yang E, Norris DA, Hanifin JM, Sampson HA. 1993. Presence of IgE antibodies to staphylococcal exotoxins on the skin of patients with atopic dermatitis: evidence for a new group of allergens. *J. Clin. Invest.* 92:1374–1380
106. Gascoigne NRJ, Ames KT. 1991. Direct binding of secreted T-cell receptor β chain to superantigen associated with class II major histocompatibility complex protein. *Proc. Natl. Acad. Sci. USA* 88:613–616
107. Malmqvist M. 1993. Surface plasmon resonance for detection and measurement of antigen–antibody affinity and kinetics. *Curr. Biol.* 5:282–286
108. Margulies DH, Plaskin D, Khilko SN, Jelonek MT. 1996. Studying interactions involving the T-cell antigen receptor by surface plasmon resonance. *Curr. Opin. Immunol.* 8:262–270
109. Seth A, Stern LS, Ottenhoff THM, Engel I, Owen MJ, Lamb JR, Klausner RD, Wiley DC. 1994. Binary and ternary complexes between T-cell receptor, class II MHC and superantigen *in vitro*. *Nature* 369:324–327
110. Malchiodi EL, Eisenstein E, Fields BA, Ohlendorf DH, Schlievert PM, Karjalainen K, Mariuzza RA. 1995. Superantigen binding to a T cell receptor β chain of known three–dimensional structure. *J. Exp. Med.* 182:1833–1845
111. Leder L, Llera A, Lavoie PM, Lebedeva MI, Li H, Sekaly R-P, Bohach GA, Gahr PJ, Schlievert PM, Karjalainen K, Mariuzza RA. 1998. A mutational analysis of the binding of staphylococcal enterotoxins B and C3 to the T cell receptor β chain and major histocompatibility complex class II. *J. Exp. Med.* 187:823–833
112. Khandekar SS, Brauer PP, Naylor JW, Chang H–C, Kern P, Newcomb JR, LeClair KP, Stump HS, Bettencourt BM, Kawasaki E, Banerji J, Profy AT, Jones B. 1997. Affinity and kinetics of the interactions between an $\alpha\beta$ T-cell receptor and its superantigen and class II–MHC/peptide ligands. *Mol. Immunol.* 34:493–503
113. van der Merwe PA, Brown MH, Davis SJ, Barclay AN. 1993. Affinity and kinetics of the interaction of the cell adhesion molecules rat CD2 and CD48. *EMBO J.* 12:4945–4954
114. van der Merwe PA, Barclay AN, Mason DW, Davis EA, Morgan BP, Tone M, Krishnam AKC, Ianelli C, Davis SJ. 1994. Human cell–adhesion molecule CD2 binds CD58 (LFA–3) with a very low affinity and an extremely fast dissociation rate but does not bind CD48 or CD59. *Biochemistry* 33:10149–10160
115. Corr M, Slanetz AE, Boyd LF, Jelonek MT, Khilko S, Al-Ramadi BK, Kim YS, Maher SE, Bothwell AL, Margulies DH. 1994. T cell receptor–MHC class I peptide interactions: affinity, kinetics, and specificity. *Science* 265:946–948
116. Matsui K, Boniface JJ, Steffner P, Reay PA, Davis MM. 1994. Kinetics of T cell receptor binding to peptide/I–E^k complexes: correlation of the dissociation rate with T-cell responsiveness. *Proc. Natl. Acad. Sci. USA* 91:12862–12866
117. Alam SM, Travers PJ, Wung JL, Nasholds W, Redpath S, Jameson SC, Gascoigne NRJ. 1996. T-cell receptor affinity and thymocyte positive selection. *Nature* 381:616–620
118. Valitutti S, Muller S, Cella M, Padovan E, Lanzavecchia A. 1995. Serial triggering of many T-cell receptors by a few peptide–MHC complexes. *Nature* 375:148–151
119. Viola A, Lanzavecchia A. 1996. T cell activation determined by T cell receptor number and tunable thresholds. *Science* 273:104–106
120. Rabinowitz JD, Beeson C, Lyons DS, Davis MM, McConnell HM. 1996. Kinetic discrimination in T-cell activation. *Proc. Natl. Acad. Sci. USA* 93:1401–1405
121. Proft T, Fraser J. 1998. Superantigens: just like peptides only different. *J. Exp. Med.* 187:819–821
122. Jardetzky TS, Brown JH, Gorga JC, Urban RG, Chi YI, Stauffacher C, Strominger JL, Wiley DC. 1994. Three–dimensional structure of a human class II histocompatibility molecule complexed with superantigen. *Nature* 368:711–718
123. Dessen A, Lawrence CM, Cupo S, Zaller DM, Wiley DC. 1997. X–ray crystal structure of HLA–DR4 (DRA*0101, DRB1*0401) complexed with a peptide from human collagen II. *Immunity* 7:473–481
124. Kim J, Urban RG, Strominger JL, Wiley DC. 1994. Toxic shock syndrome toxin–1 complexed with a class II major histocompatibility molecule HLA–DR1. *Science* 266:1870–1874
125. Mollick JA, Chintagumpala M, Cook RG, Rich RR. 1991. Staphylococcal exotoxin activation of T-cells. Role of exotoxin–MHC class II binding affinity and class II isotype. *J. Immunol.* 146:463–468
126. Wen R, Cole GA, Surman S, Blackman MA, Woodland DL. 1996. Major histocompatibility complex class II–associated peptides control the presentation of

bacterial superantigens to T cells. *J. Exp. Med.* 183:1083–1092
127. Kozono H, Parker D, White J, Marrack P, Kappler J. 1995. Multiple binding sites for bacterial superantigens on soluble class II molecules. *Immunity* 3:187–196
128. Hudson KR, Tiedemann RE, Urban RG, Lowe SC, Strominger JL, Fraser JD. 1995. Staphylococcal enterotoxin A has two cooperative binding sites on major histocompatibility complex class II. *J. Exp. Med.* 182:711–720
129. Abrahmsen L, Dohlsten M, Segren S, Bjork P, Jonsson E, Kalland T. 1995. Characterization of two distinct MHC class II binding sites in the superantigen staphylococcal enterotoxin A. *EMBO J.* 14:2978–2986
130. Tiedemann RE, Urban RJ, Strominger JL, Fraser JD. 1995. Isolation of HLA–DR1.(staphylococcal enterotoxin A)2 trimers in solution. *Proc. Natl. Acad. Sci. USA* 92:12156–12159
131. Mehindate K, Thibodeau J, Dohlsten M, Kalland T, Sekaly R–P, Mourad W. 1995. Cross–linking of major histocompatibility complex class II molecules by staphylococcal enterotoxin A is a requirement for inflammatory cytokine gene expression. *J. Exp. Med.* 182:1573–1577
132. Tiedemann RE, Fraser JD. 1996. Cross–linking of MHC class II molecules by staphylococcal enterotoxin A is essential for antigen–presenting cell and T cell activation. *J. Immunol.* 157:3958–3966
133. Winslow GM, Marrack P, Kappler JW. 1994. Processing and major histocompatibility complex binding of the MTV7 superantigen. *Immunity* 1:23–33
134. Mottershead DG, Hsu P–N, Urban RG, Strominger JL, Huber BT. 1995. Direct binding of the Mtv7 superantigen (Mls–1) to soluble MHC class II molecules. *Immunity* 2:149–154
135. Held W, Waanders GA, MacDonald HR, Acha–Orbea H. 1994. MHC class II hierarchy of superantigen presentation predicts efficiency of infection with mouse mammary tumor virus. *Int. Immunol.* 6:1403–1407
136. Pucillo C, Cepeda R, Hodes RJ. 1993. Expression of a MHC class II transgene determines superantigenicity and susceptibility to mouse mammary tumor virus infection. *J. Exp. Med.* 178:1441–1445
137. Thibodeau J, Labrecque N, Denis F, Huber BT, Sekaly R–P. 1994. Binding sites for bacterial and endogenous retroviral superantigens can be dissociated on major histocompatibility complex class II molecules. *J. Exp. Med.* 179:1029–1034
138. Torres BA, Griggs ND, Johnson HM. 1993. Bacterial and retroviral superantigens share a common binding region on class II MHC antigens. *Nature* 364:152–154
139. McMahon CW, Bogatzki LY, Pullen AM. 1997. Mouse mammary tumor virus superantigens require N–linked glycosylation for effective presentation to T cells. *Virology* 228:161–170
140. Labrecque N, Thibodeau J, Mourad W, Sekaly R–P. 1994. T cell receptor–major histocombatibility complex class II interaction is required for the T cell response to bacterial superantigens. *J. Exp. Med.* 180:1921–1929
141. Deckhut AM, Chien Y, Blackman MA, Woodland DL. 1994. Evidence for a functional interaction between the β chain of major histocompatibility complex class II and the T cell receptor α chain during recognition of a bacterial superantigen. *J. Exp. Med.* 180:1931–1935
142. Blackman MA, Woodland DL. 1996. Role of the T cell receptor α–chain in superantigen recognition. *Immunol. Res.* 15:98–113
143. Padlan EA. 1994. Anatomy of the antibody molecule. *Mol. Immunol.* 31:169–217
144. Fremont DH, Matsumura M, Stura EA, Peterson PA, Wilson IA. 1992. Crystal structures of two viral peptides in complex with MHC class I H–$2K^b$. *Science* 257:919–927
145. Madden D. 1995. The three–dimensional structure of peptide–MHC complexes. *Annu. Rev. Immunol.* 13:587–622
146. Bhat TN, Bentley GA, Boulot G, Greene MI, Tello D, Dall'Acqua W, Souchon H, Schwarz FP, Mariuzza RA, Poljak RJ. 1994. Bound water molecules and conformational stabilization help mediate an antigen–antibody association. *Proc. Natl. Acad. Sci. USA* 91:1089–1093
147. Fields BA, Goldbaum FA, Ysern X, Poljak RJ, Mariuzza RA. 1995. Molecular basis of antigen mimicry by an anti–idiotope. *Nature* 374:739–742
148. Dall'Acqua W, Goldman ER, Lin W, Teng C, Tsuchiya D, Li H, Ysern X, Braden BC, Li Y, Smith-Gill SJ, Mariuzza RA. 1998. A mutational analysis of binding interactions in an antigen–antibody protein–protein complex. *Biochemistry* 37:7981–7991
149. Hodtsev AS, Choi Y, Spanopoulou E, Posnett DN. 1998. Mycoplasma superantigen is a CDR3–dependent ligand for the T cell antigen receptor. *J. Exp. Med.* 187:319–327

150. Ciurli C, Posnett DN, Sekaly R–P, Denis F. 1998. Highly biased CDR3 usage in restricted sets of β chain variable regions during viral superantigen 9 response. *J. Exp. Med.* 187:253–258
151. Hong S–C, Waterbury G, Janeway CA Jr. 1996. Different superantigens interact with distinct sites in the Vβ domain of a single T cell receptor. *J. Exp. Med.* 183:1437–1446
152. Davies DR, Padlan EE. 1992. Twisting into shape. *Curr. Biol.* 2:254–256
153. Tulip WR, Varghese JN, Laver WG, Webster RG, Coleman PM. 1992. Refined crystal structure of the influenza virus N9 neuraminidase–NC41 Fab complex. *J. Mol. Biol.* 227:122–148
154. Wilson IA, Stanfield RL. 1993. Antigen–antibody interactions. *Curr. Opin. Struct. Biol.* 3:113–118
155. Lawrence MC, Coleman PM. 1993. Shape complementarity at protein/protein interfaces. *J. Mol. Biol.* 234:946–950
156. Ysern X, Li H, Mariuzza RA. 1998. Imperfect interfaces. *Nature Struct. Biol.* 5:412–414
157. Reich Z, Boniface JJ, Lyons DS, Borochov N, Wachtel EJ, Davis MM. 1997. Ligand–specific oligomerization of T-cell receptor molecules. *Nature* 387:617–620
158. Imanishi KH, Igarashi H, Uchiyama T. 1990. Activation of murine T cells by streptococcal pyrogenic exotoxin A. *J. Immunol.* 145:3170–3176
159. Woodland DL, Blackman MA. 1993. How do T cell receptors, MHC molecules and superantigens get together? *Immunol. Today* 14:208–212
160. Borrero H, Donson D, Cervera C, Rexer C, Macphail S. 1995. T cell receptor Vα4 is expressed by a subpopulation of Vβ6 T cells that respond to the bacterial superantigen staphylococcal enterotoxin B. *J. Immunol.* 154:4247–4260
161. Donson D, Borrero H, Rutman M, Pergolizzi R, Malhado N, Macphail S. 1997. Gene transfer directly demonstrates a role for TCR Vα elements in superantigen recognition. *J. Immunol.* 158:5229–5236
162. Daly K, Nguyen P, Hankley D, Zhang WJ, Woodland DL, Blackman MA. 1995. Contribution of the TCR α–chain to the differential recognition of bacterial and retroviral superantigens. *J. Immunol.* 155:27–34
163. Abrahmsén L. 1995. Superantigen engineering. *Curr. Opin. Struct. Biol.* 5:464–470
164. Dohlsten M, Hedlund G, Åkerblom E, Lando PA, Kalland T. 1991. Monoclonal antibody–targeted superantigens: A different class of anti–tumor agents. *Proc. Natl. Acad. Sci. USA* 88:9287–9291
165. Dohlsten M, Abrahmsén L, Björk P, Lando PA, Hedlund G, Forsberg G, Brodin T, Gascoigne NRJ, Förberg C, Lind P, Kalland T. 1994. Monoclonal antibody–superantigen fusion proteins: Tumor–specific agents for T-cell–based tumor therapy. *Proc. Natl. Acad. Sci. USA* 91:8945–8949
166. Ihle J, Holzer U, Krull F, Dohlsten M, Kalland T, Niethammer D, Dannecker GE. 1995. Antibody–targeted superantigens induce lysis of major histocompatibility complex class II–negative T-cell leukemia lines. *Cancer Res.* 55:623–628
167. Holzer U, Bethge W, Krull F, Ihle J, Handgretinger R, Reisfeld RA, Dohlsten M, Kalland T, Niethammer D, Dannecker GE. 1995. Superantigen–staphylococcal–enterotoxin–A–dependent and antibody–targeted lysis of GD2–positive neuroblastoma cells. *Cancer Immunol. Immunother.* 41:129–136
168. Hansson J, Ohlsson L, Persson R, Andersson G, Ilbäck N–G, Litton MJ, Kalland T, Dohlsten M. 1997. Genetically engineered superantigens as tolerable antitumor agents. *Proc. Natl. Acad. Sci. USA* 94:2489–2494
169. Giantonio BJ, Alpaugh RK, Schultz J, McAleer C, Newton DW, Shannon B, Guedez Y, Kotb M, Vitek L, Persson R, Gunnarsson PO, Kalland T, Dohlsten M, Persson B, Weiner LM. 1997. Superantigen–based immunotherapy: a phase I trial of PNU–214565, a monoclonal antibody–staphylococcal enterotoxin A recombinant fusion protein, in advanced pancreatic and colorectal cancer. *J. Clin. Oncol.* 15:1994–2007
170. Kappler JW, Herman A, Clements J, Marrack P. 1992. Mutations defining functional regions of the superantigen staphylococcal enterotoxin B. *J. Exp. Med.* 175:387–396
171. Bavari S, Dyas B, Ulrich RG. 1996. Superantigen vaccines: a comparative study of genetically attenuated receptor–binding mutants of staphylococcal enterotoxin A. *J. Infect. Dis.* 174:338–345
172. Tseng J, Komisar JL, Trout RN, Hunt RE, Chen JY, Johnson AJ, Pitt L, Ruble DL. 1995. Humoral immunity to aerosolized staphylococcal enterotoxin B (SEB), a superantigen, in monkeys vaccinated with SEB toxoid–containing microspheres. *Infect. Immun.* 63:2880–2885
173. Lowell GH, Colleton C, Frost D, Kaminski RW, Hughes M, Hatch J,

Hooper C, Estep J, Pitt L, Topper M, Hunt RE, Baker W, Baze WB. 1996. Immunogenicity and efficacy against lethal aerosol staphylococcal enterotoxin B challenge in monkeys by intramuscular and respiratory delivery of proteosome–toxoid vaccines. *Infect. Immun.* 64:4686–4693

174. McCormack JE, Callahan JE, Kappler J, Marrack PC. 1993. Profound deletion of mature T cells in vivo by chronic exposure to exogenous superantigen. *J. Immunol.* 150:3785–3792
175. Miethke T, Wahl C, Heeg K, Wagner H. 1993. Acquired resistance to superantigen–induced T cell shock. Vβ selective T cell unresponsiveness unfolds directly from a transient state of hyperreactivity. *J. Immunol.* 150:3776–3784
176. Kim C, Siminovitch KA, Ochi A. 1991. Reduction of lupus nephritis in MRL/lpr mice by a bacterial superantigen treatment. *J. Exp. Med.* 174:1431–1437
177. Rott O, Wekerle H, Fleischer B. 1992. Protection from experimental allergic encephalomyelitis by application of a bacterial superantigen. *Int. Immunol.* 4:347–353
178. Soos JM, Schiffenbauer J, Johnson HM. 1993. Treatment of PL/J mice with superantigen staphylococcal enterotoxin B, prevents development of experimental allergic encephalomyelitis. *J. Neuroimmunol.* 43:39–43
179. Racke MK, Quigley L, Cannella B, Raine C, McFarlin DE, Scott DE. 1994. Superantigen modulation of experimental allergic encephalomyelitis: activation or anergy determines outcome. *J. Immunol.* 152:2051–2059
180. Leung DYM, Schlievert PM. 1997. Superantigens in human disease. In *Superantigens: Molecular Biology, Immunology and Relevance to Human Disease*, ed. DYM Leung, BT Huber, PM Schlievert, Marcel Dekker Inc. NY, pp. 581–601
181. Hurley JM, Shimonkevitz R, Hanagan A, Enney K, Boen E, Malmstron S, Kotzin BL, Matsumura M. 1995. Identification of class II major histocompatibility complex and T cell receptor binding sites in the superantigen toxic shock syndrome toxin–1. *J. Exp. Med.* 181:2229–2235
182. Murray DL, Prasad GS, Earhart CA, Leonard BAB, Kreiswirth BN, Novick RP, Ohlendorf DH, Schlievert PM. 1994. Immunobiologic and biochemical properties of mutants of toxic shock syndrome toxin–1. *J. Immunol.* 152:87–95
183. Deresiewicz RL, Wood J, Chan M, Finberg RW, Kasper DL. 1994. Mutations affecting the activity of toxic shock syndrome toxin–1. *Biochemistry* 33:12844–12851

Annual Review of Immunology
Volume 17, 1999

CONTENTS